



저작자표시-비영리-변경금지 2.0 대한민국

이용자는 아래의 조건을 따르는 경우에 한하여 자유롭게

- 이 저작물을 복제, 배포, 전송, 전시, 공연 및 방송할 수 있습니다.

다음과 같은 조건을 따라야 합니다:



저작자표시. 귀하는 원저작자를 표시하여야 합니다.



비영리. 귀하는 이 저작물을 영리 목적으로 이용할 수 없습니다.



변경금지. 귀하는 이 저작물을 개작, 변형 또는 가공할 수 없습니다.

- 귀하는, 이 저작물의 재이용이나 배포의 경우, 이 저작물에 적용된 이용허락조건을 명확하게 나타내어야 합니다.
- 저작권자로부터 별도의 허가를 받으면 이러한 조건들은 적용되지 않습니다.

저작권법에 따른 이용자의 권리는 위의 내용에 의하여 영향을 받지 않습니다.

이것은 [이용허락규약\(Legal Code\)](#)을 이해하기 쉽게 요약한 것입니다.

[Disclaimer](#)

농학박사학위논문

붉은 곰팡이 바이러스 1 과
상호작용하는 붉은 곰팡이의 *HEX1*
유전자에 대한 기능분석연구

**Functional analysis of *HEX1* gene in interaction
between *Fusarium graminearum* and
Fusarium graminearum virus 1**

2015년 2월

서울대학교 대학원

농생명공학부 식물미생물학

손문일

Functional analysis of *HEX1* gene in interaction
between *Fusarium graminearum* and

Fusarium graminearum virus 1

A dissertation submitted in partial
fulfillment of the requirement for
the degree of

DOCTOR OF PHILOSOPHY

to the Faculty of
Department of Agricultural Biotechnology
at

SEOUL NATIONAL UNIVERSITY

by

Moonil Son

February 2015

농학박사학위논문

붉은 곰팡이 바이러스 1과 상호작용하는
붉은 곰팡이의 *HEXI* 유전자에 대한 기능분석 연구

지도교수 김 국 형

이 논문을 농학박사학위논문으로 제출함

2015년 2월

서울대학교 대학원

농생명공학부 식물미생물학 전공

손문일

손문일의 박사학위논문을 인준함

2015년 2월

위원장	_____	(인)
부위원장	_____	(인)
위원	_____	(인)
위원	_____	(인)
위원	_____	(인)

A THESIS FOR THE DEGREE OF DOCTOR OF PHILOSOPHY

Functional analysis of *HEX1* gene in interaction
between *Fusarium graminearum* and
Fusarium graminearum virus 1

UNDER THE DIRECTION OF DR. KOOK-HYUNG KIM
SUBMITTED TO THE FACULTY OF THE GRADUATE SCHOOL
OF SEOUL NATIONAL UNIVERSITY

BY
MOONIL SON

MAJOR IN PLANT MICROBIOLOGY
DEPARTMENT OF AGRICULTURAL BIOTECHNOLOGY

FEBRUARY 2015

APPROVED AS A QUALIFIED THESIS OF MOONIL SON
FOR THE DEGREE OF DOCTOR OF PHILOSOPHY
BY THE COMMITTEE MEMBERS

CHAIRMAN _____

VICE CHAIRMAN _____

MEMBER _____

MEMBER _____

MEMBER _____

**Functional analysis of *HEX1* gene in interaction
between *Fusarium graminearum* and
Fusarium graminearum virus 1**

Moonil Son

ABSTRACT

Fusarium graminearum virus 1 strain DK21 (FgV1) is fungal virus (mycovirus) isolated from the devastating plant pathogenic fungi, *Fusarium graminearum*. The FgV1 genome consists of 6,624 nucleotides, excluding the 3'-terminal poly (A) tail. The viral genome has 53- and 46-nucleotide 5'-and 3'-untranslated regions (UTRs), respectively, and four putative open reading frames. The FgV1 infection perturbs in various aspects of host fungus biology such as morphology, growth, development, metabolism, and even virulence to plant. To identify a certain host factor interacting with FgV1 which involves in such alteration of host, proteome and transcriptome based approaches have been tried previously. Among them, the hexagonal peroxisome (Hex1) protein is fungal protein that is highly expressed when FgV1 infects its host. The Hex1 protein constitutes Woronin body (WB),

which is peroxisome derived dense-core micro organelle for sealing the septal pore in response to hyphal damage. In the present study, cellular functions of Hex1 in *F. graminearum* and particular function for FgV1 were characterized. First, in order to investigate roles of Hex1, *HEX1* gene deletion, over-expression and complementation mutants were generated and then infected by FgV1. Deletion and over-expression of Hex1 did not affect to vegetative growth in virus-free (VF) strains, while both changes resulted in reduced production of conidia and reduced virulence. Additionally, fungal cells could not maintain cellular integrity after hyphal wounding in the absence of *HEX1* gene and even they showed cytoplasmic bleeding. Taken together, combined results suggested that *HEX1* gene is required for asexual reproduction and pathogenesis and maintaining cellular integrity. Although deletion and over-expression did not affect vegetative growth at all in VF strains, both genetic alterations substantially affected vegetative growth in virus-infected (VI) strains. Vegetative growth was increased in deletion strains and decreased in over-expression strains comparing with WT-VI strain, while viral RNA accumulation was decreased in deletion strains and increased in over-expression strain. To clarify the cause of these different RNA accumulations in different *HEX1* strains, FgV1 and Hex1 interaction studies were carried out. Homology based protein tertiary structure

prediction analysis demonstrated that the structure of Hex1 is similar to that of eukaryotic translational initiation factor 5A (IF-5A) which have RNA-binding folds on its surface. Therefore, I carried out electrophoretic mobility shift assays (EMSAs) and the analysis revealed Hex1 protein bind to both 5'-and 3'-untranslated regions (UTRs) of plus-strand viral RNA. Strand specific Northern blot and qRT-PCR analyses were conducted to determine the effect of Hex1 on FgV1 (+)- and (-)-strand RNA accumulation. Both analyses exhibited that Hex1 protein affected both (+)- and (-)-strand RNA accumulations.

Keywords: *Fusarium graminearum* virus 1, *Fusarium graminearum*, Hex1 protein, host factor, RNA-protein binding, viral RNA replication

Student number: 2008-21357

CONTENTS

	<i>page</i>
ABSTRACT	i
CONTENTS	iv
LIST OF TABLES	ix
LIST OF FIGURES	x
 GENERAL INTRODUCTION	
	<i>page</i>
I. Mycovirus	14
II. Hypovirulence associated mycoviruses	15
III. Isolation of mycoviruses from <i>Fusarium graminearum</i>	16
IV. <i>Fusarium graminearum</i> virus 1	17
V. Identification of fungal host factors in response to FgV1 ..	18
VI. Fungal host factor Hex1	21
VII. Hex1 and FgV1 interaction studies in this work	22
 LITERATURE CITED	 23

CHAPTER I. The *HEX1* gene of *Fusarium graminearum* is required for fungal asexual reproduction and pathogenesis and for efficient viral RNA accumulation of *Fusarium graminearum* virus 1

	<i>page</i>
ABSTRACT	28
INTRODUCTION	30
MATERIALS AND METHODS	
I. Fungal strains and culture condition	34
II. Computational analysis	34
III. Genomic DNA extraction, primers, and PCR conditions	35
IV. Fungal transformation for construction of targeted gene-deletion, over-expression, and complementation mutants.....	36
V. Radial growth, conidial production, and virulence test	37
VI. Observation of WB formation using electron microscopy	38
VII. Measurement of intercalary length	39
VIII. Fungal protein extraction and western blot analysis	40
IX. RNA preparation and RT-PCR	41

RESULTS

I. Sequence analysis of <i>F. graminearum</i> <i>HEX1</i> and homologs from other plant-pathogenic fungi	44
II. Targeted deletion, over-expression, and complementation of the <i>HEX1</i> gene	47
III. Colony morphology and vegetative growth of <i>HEX1</i> mutants.....	50
IV. Conidial production.....	52
V. Subcellular localization of WBs and western blot analysis.....	55
VI. Functions of the <i>HEX1</i> gene with respect to the maintenance of cellular integrity and pathogenesis	55
VII. Quantification of <i>HEX1</i> gene expression	58
VIII. Quantification of FgV1 viral RNA accumulation.....	62

DISCUSSION	68
------------------	----

LITERATURE CITED	77
------------------------	----

CHAPTER II. Hex1 protein binds specifically to both plus-strand 5'-and 3'-untranslated regions of the Fusarium graminearum virus 1 and functions in virus RNA replication.

	<i>page</i>
ABSTRACT	87
INTRODUCTION	88
 MATERIALS AND METHODS	
I. Fungal strains and culture conditions	91
II. Computational analysis	91
III. Preparation of protoplast and total RNA extraction	92
IV. Plasmid construction and RNA transcription	93
V. Hex1 protein expression in <i>E. coli</i>	94
VI. Electrophoretic mobility shift assays	94
VII. Fungal protein extraction and western blot analysis	95
VIII. qRT-PCR and Northern blot analysis	96

RESULTS

I. Structure of Hex1 protein and homology with eIF-5A	99
II. Purification of Hex1 protein from <i>E. coil</i> and western blot analysis	99
III. Plasmid construction and Hex1 protein manipulation	102
IV. Specific binding of Hex1 to both 5' and 3' UTR of FgV1 plus-strand RNA	104
V. Strand specific quantification of FgV1 viral RNA accumulation	107
VI. Effect of Hex1 on strand specific RNA synthesis in protoplast	111

DISCUSSION	115
-------------------------	-----

LITERATURE CITED	122
-------------------------------	-----

ABSTRACT (in Korea)	129
----------------------------------	-----

ACKNOWLEDGEMENTS	133
-------------------------------	-----

LIST OF TALBLES

CHAPTER I

page

Table 1. Fungal strains used in this study43

Table 2. Average intercalary lengths (= cell length) of the HEX1 mutants..67

CHAPTER II

Table 1. Fungal strains used in this study.....98

LIST OF FIGURES

GENERAL INTRODUCTION

page

Fig. 1. Genome organization of <i>Fusarium graminearum</i> virus 1	19
---	----

CHAPTER I

page

Fig. 1. Phylogenetic tree of predicted amino acid sequences of <i>HEX1</i> homologs	45
Fig. 2. Deduced amino acid sequence alignment with closely related plant-pathogenic fungi	46
Fig. 3. Construction strategy of <i>HEX1</i> gene-deletion, over-expression, and complementation mutants in <i>F. graminearum</i>	48
Fig. 4. Southern blot hybridization	49
Fig. 5. Colony morphology of mutants	51
Fig. 6. Radial growth after 5 days on PDA	53
Fig. 7. Conidial production after 5 days in CMC liquid medium	54
Fig. 8. Subcellular localization of Woronin bodies (WBs)	56

Fig. 9. Western blot analysis using Hex1 antibody in the <i>HEX1</i> mutants	57
Fig. 10. Growth of hyphae of WT-VF, $\Delta hex1$ -VF, HEX OE-VF, and $\Delta hex1::HEX1$ -VF strains after amputation with a razor blade	59
Fig. 11. Cytoplasmic bleeding in the <i>HEX1</i> deletion strain	60
Fig. 12. Virulence assay with <i>HEX1</i> mutants and the wild type (WT) of <i>F. graminearum</i> that were infected with FgV1 (indicated by VI) or virus free (indicated by VF)	61
Fig. 13. qRT-PCR analysis of expression of <i>HEX1</i> and its orthologs in <i>F. graminearum</i> and <i>Cryphonectria parasitica</i> as affected by mycovirus infection	63
Fig. 14. Quantification of FgV1 viral RNA accumulation in <i>F. graminearum</i> using qRT-PCR	64
Fig. 15. Quantification of FgV1 viral RNA accumulation in <i>F. graminearum</i> using sqRT-PCR	66

CHAPTER II

page

Fig. 1. Deduced amino acid sequence alignment of Hex1 from <i>N. crassa</i> (NcHex1), <i>F. graminearum</i> (FgHex1) and IF-5A from <i>F. graminearum</i> (FgIF5A), <i>P. aerophilum</i> (PaIF5A), <i>M. jannaschii</i> (MjIF5A)	100
Fig. 2. Predicted structures of Hex1 and IF-5A	101
Fig. 3. <i>E. coli</i> expression of Hex1 and western blot analysis	103
Fig. 4. Construction of plasmid and Hex1 protein manipulation	105
Fig. 5. Investigation of direct interaction using RNA-protein complexes formation	106
Fig. 6. Relative free RNA probes in EMSA experiments	108
Fig. 7. Electrophoretic mobility shift assay (EMSA) of FgV1 RNA-Hex1 protein complex	109
Fig. 8. Plus- and minus-strand RNA accumulation in all virus-infected strains	110
Fig. 9. Relative plus- and minus-strand viral RNA accumulation in all virus-infected strains of <i>F.graminearum</i>	112
Fig. 10. Time course mediated quantification of FgV1 viral RNA replication in virus-infected <i>F. graminearum</i> protoplasts	113

Fig. 11. Relative plus- and minus-strand viral RNA accumulation in all	
virus-infected protoplasts	114

GENERAL INTRODUCTION

I. Mycovirus

Mycoviruses are fungal viruses that infect almost all major groups of fungi. Studies which have been elucidated mycovirus are relatively poor as compared to those of animal and plant. However, our knowledge and understandings about mycovirus have been accumulated over the time through ceaseless efforts of research groups all over the world.

The first mycovirus is discovered in cultivated mushrooms, *Agaricus bisporus*. Infected mushrooms showed malformation of fruiting body, slow growth, premature maturation and serious yield loss (Hollings et al., 1962). The disease called La France, and similar diseases in Japan, Australia, and Europe were also reported thereafter. Subsequently, several decades of researches have been provided more insight of mycoviruses (Ghabrial and Suzuki, Pearson et al., 2009).

In general, mycovirus have either double-stranded (ds) or single-stranded (ss) RNA genomes. Recently, mycovirus which has ssDNA as a genome is reported and characterized (Yu et al., 2010). Including virus-like particles and unencapsidated dsRNAs, mycoviruses are composed of 90 species which are officially recognized from ten virus families according to the

updated 9th ICTV report on virus taxonomy (King et al., 2011).

Mycoviruses exist commonly in fungi and are detected in all four phyla of the true fungi: *Chytridiomycota*, *Zygomycota*, *Ascomycota*, and *Basidiomycota* (Herrero et al., 2009). All fungi in these groups are the host of at least two or more unrelated mycoviruses, respectively. Therefore, at this very moment, the host range of mycovirus is expanding. Furthermore, there was an attempt to extend the natural host range of *Cryphonectria hypovirus 1* (CHV1) from *Cryphonectria parasitica*, as an original host, to several fungal species using *in vitro* transfection technique (Nuss et al., 2005). Recently, it has also reported that *Fusarium graminearum virus 1* can be successfully transmitted to *C. parasitica* and other *Fusarium* species via protoplast fusion technique and propagated well (Lee et al., 2011).

Although the origin of mycovirus is not well defined, recently provided data proposed two different hypotheses: 1) ancient coevolution hypothesis is based on bidirectional influences between fungal host and mycovirus over the time and 2) the plant virus hypothesis explaining that mycovirus are moved from a fungal plant host into the fungus. (Pearson et al., 2009).

II. Hypovirulence of myvirus

Many mycoviruses are widespread throughout the major taxonomic

groups of fungi, most of mycoviruses are cryptic effect (non-symptomatic) or latent (expressed only under some special conditions). However, some mycoviruses showed distinct characteristic, affecting the host biology during infection even at the molecular level. Among these alterations, some mycoviruses confer hypovirulence (mycovirus mediated attenuation of fungal virulence) to their host (Nuss et al., 2005).

The best characterized examples of mycoviruses that have hypovirulence trait are hypoviruses of the chestnut blight fungus, *C. parasitica*. Among them, CHV1 has been dominated in the context of plant pathology and it has been used as a biological control agent for chestnut blight (Ghabrial et al., 2009).

III. Identification of dsRNA mycoviruses isolated from *Fusarium*

graminearum

Many mycoviruses infecting *F. graminearum* have been identified and characterized globally using large-scale screening (for a review see Cho et al., 2013). Among the previous researches, the 827 *F. graminearum* isolates which isolated from diseased barely and maize in Korea had 19 dsRNA fragments (Chu et al., 2004). Among these 19 isolates, dsRNA element from 3 strains such as strain DK21, 98-8-60, and DK3 were successfully analyzed

using various molecular tools (Chu et al., 2002, Kwon et al., 2007, Yu et al., 2009 and 2011) Recently, in China, *Fusarium graminearum* virus-ch9 (FgV-ch9) was isolated and consist of at least five dsRNA fragments (Darissa et al., 2011). In Iran, at least 12 of 33 isolates contained three different dsRNA fragments which ranged in size from 0.9 to 5 kb (Aminian et al., 2011)

IV. *Fusarium graminearum* virus 1 (FgV1)

From previous studies in year 2002 and 2004, one dsRNA mycovirus isolated from strain DK21 showed distinguishable features comparing with other isolates and then identified *Fusarium graminearum* virus-DK21 (currently named *Fusarium graminearum* virus 1, FgV1). When fungal host infected FgV1, the fungi showed reduced virulence on wheat, hypovirulence. Additionally, delayed mycelial growth, increased pigmentation and reduced mycotoxin production. Moreover, phylogenetic analysis using amino acid sequence revealed that RNA-dependent RNA polymerase protein sequence of FgV1 is closed related that of *Cryphonectria hypovirus* 1 (Chu et al., 2002 and 2004).

The FgV1 viral genome is 6624-bp long and contains four open reading frames (ORFs). FgV1 has 5'-and 3'-untranslated regions (UTRs) with

lengths 52 and 46 bp, respectively (Fig. 1). Amino acid alignment with other reported mycovirus, only ORF1 is predicted as RNA-dependent RNA polymerase and similar with those of *Cryphonectria* hypoviruses and barley yellow mosaic virus (BaYMV) while the other three ORFs do not match any sequence of other viruses (Kwon et al., 2007).

V. Identification of fungal host factors interacting with FgV1

Similar with the animal and plant virus, the mycovirus is also obligate parasite that depends on host cell for successful propagation. In infection, mycovirus should exploit and usurp cellular machinery through various interactions such as protein-protein, protein-RNA and protein-lipid interactions. The molecular mechanism between virus and host factor is never-ending process in all viral life cycle and decide host range, virus pathogenesis and even virus evolution (Wang et al., 2011). Therefore, study about host factor can provide insights of their original cellular functions and the viral life in host cell. In accordance with molecular technologies such as high-throughput screening, functional genomics and proteomic technologies, host factor involved in viral life has been reported rapidly in recent years

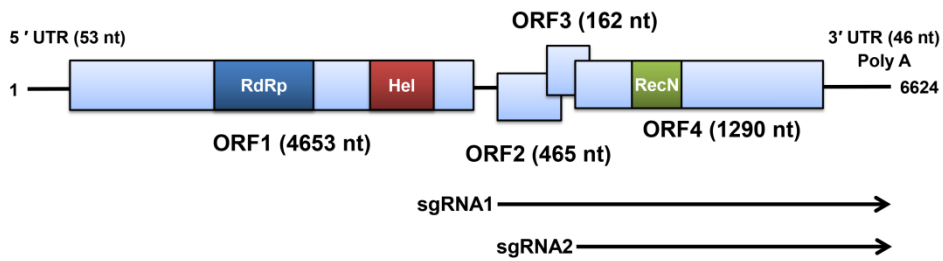


Fig. 1. Genome organization of FgV1. FgV1 is consisted only one genomic RNA containing putative four ORFs. ORF3 initiation codon overlaps termination codon of ORF2 in the tetranucleotide (AUGA). ORF4 initiation codon also overlaps termination codon of ORF3 in the tetranucleotide (AUGA). FgV1 uses at least two subgenomic RNAs to express putative ORFs. The black line indicates the length of nucleotide for each RNA. The sizes of 5'-UTR, 3'-UTR and ORFs are also indicated as nucleotides. The names of each protein motifs are as follow: RdRp for RNA-dependent RNA polymerase and Hel for Helicase in ORF1, RecN for DNA repair protein.

(Son et al., 2013)

There had been several reports on identifying fungal host factor which respond to FgV1 infection. One of the efforts employed two-dimensional gel electrophoresis (2-DE) with mass spectrometry. By comparing 2-DE gels from two different fungal total proteins derived from virus-free (VF) and virus-infected (VI) strain, 148 spots were identified indicating differential expression between VF and VI strain. Among 148 spots, 33 were further selected for ESI-MS/MS analysis. As a result, 23 fungal proteins were identified that 7 proteins are highly expressed while other 16 protein are down-regulated by FgV1 infection (Kwon et al., 2009).

As a continued series for identification of host factor upon FgV1, 3'-tiling microarray was performed that can cover whole gene of *F. graminearum* (13,382 genes). From this study, one could easily compare global transcriptional changes by VF and VI at different time points such as 36 h and 120 h. Expression of fungal-specific transcription factors (TFs) were also identified using this approach (Cho et al., 2012).

Recently, an RNA-Seq based analysis of the host transcriptome identified four different transcriptomes, which infected with one of the four mycoviruses such as FgV1, FgV2, FgV3 and FgV4, respectively. According to the analysis, fungal transcriptomes were more affected by FgV1 and

FgV4 infection than by FgV2 and FgV3. Mycological phenotypes induced by four mycovirus in *F. graminearum* with transcriptional pattern were also compared (Lee et al., 2014). Taken together, these studies provide more detailed insights into host factors which involved in interaction between mycovirus and host fungus.

VI. Fungal host factor, Hex1

A recent study about individual fungal host factor for FgV1, Hex1 protein, was demonstrated original function of host protein and specific function to FgV1. Hex1 protein is one of the highly expressed proteins upon FgV1 infection derived from our previous proteomic analysis (Kwon et al., 2009). Cellular functions of Hex1 were already described in *Neurospora crassa* and *Magnaporthe oryzae* intensively. Hex1 protein (another named as woronin body major protein) consist of woronin body by self-assembly, small dense-core microbody, which is unique organelle in filamentous fungi. This woronin body was known for sealing septal pore when cellular damage was occurred (Jedd et al., 2000 and Yuan et al., 2003). In *M. oryzae*, *HEX1* deletion led to reduced virulence as compared to wild-type (Soundararajan et al., 2004). In my study about *HEX1*, I confirmed the result from previous studies and also demonstrated that deletion of *HEX1* gene resulted in

reduced conidia production. Additionally, I generated *HEX1* over-expression mutant using promoter switching to strengthen our results. In aspect of host factor for FgV1, *HEX1* is required for efficient viral RNA accumulation (Son et al., 2013).

VII. FgV1 and Hex1 interaction studies in this work

In the second chapter of my thesis, RNA–protein interaction study between FgV1 RNA fragments and Hex1 protein was conducted to characterize the functions of Hex1 proteins. First, I investigated whether Hex1 protein bind to various region of FgV1 RNA. As a result, Hex1 protein can bind to both 5'-and 3'-UTRs of plus-strand FgV1 RNAs, exclusively. Second, I also investigated the accumulation levels of both plus- and minus- RNA of FgV1 in protoplast. I found that only plus-strand RNA was increased rapidly in *HEX1* over-expression strain using time-course experiments. Taken together, these combined data suggested that specific binding of Hex1 to both 5'-and 3'-UTRs of plus-strand FgV1 RNA affected to virus replication (Son et al., 2014, unpublished).

LITERATURE CITED

- Aminian, P., Azizollah, A., Abbas, S. and Naser, S. (2011) Effect of double-stranded RNAs on virulence and deoxynivalenol production of *Fusarium graminearum* isolates. *J. Plant Protect. Res.* 51, 29-37.
- Cho, W.-K., Lee, K.-M., Yu, J., Son, M. and Kim, K.-H. (2012) Insight into mycoviruses infecting *Fusarium* species. *Adv. Virus Res.* 86, 273-288.
- Cho, W.-K., Yu, J., Lee, K.-M., Son, M., Min, K., Lee, Y.-W. and Kim, K.-H. (2012) Genome-wide expression profiling shows transcriptional reprogramming in *Fusarium graminearum* by *Fusarium graminearum* virus 1-DK21 infection. *BMC Genomics*, 13, 173.
- Chu, Y. M., Jeon, J. J., Yea, S. J., Kim, Y. H., Yun, S. H., Lee, Y.-W. and Kim, K.-H. (2002) Double-Stranded RNA Mycovirus from *Fusarium graminearum*. *Appl. Environ. Microbiol.* 68, 2529-2534.
- Chu, Y.-M., Lim, W.-S., Yea, S. J., Cho, J.-D., Lee, Y.-W. and Kim, K.-H. (2004) Complexity of dsRNA mycovirus isolated from *Fusarium graminearum*. *Virus Gene*, 28, 135-143.

- Herrero, N., Márquez, S. S. and Zabalgogezcoa, I. (2009) Mycoviruses are common among different species of endophytic fungi of grasses. *Arch. Virol.* 154, 327-330.
- Hollings, M. (1962) Viruses associated with a die-back disease of cultivated mushroom. *Nature*, 196, 962-965.
- Jedd, G. and Chua, N. H. (2000) A new self-assembled peroxisomal vesicle required for efficient resealing of the plasma membrane. *Nat. Cell Biol.* 2, 226-231.
- Kwon, S.-J., Cho, S.-Y., Lee, K.-M., Yu, J., Son, M. and Kim, K.-H. (2009) Proteomic analysis of fungal host factors differentially expressed by *Fusarium graminearum* infected with *Fusarium graminearum* virus-DK21. *Virus Res.* 144, 96-106.
- Kwon, S.-J., Lim, W.-S., Park, S.-H., Park, M.-R. and Kim, K.-H. (2009) Molecular characterization of a dsRNA mycovirus, *Fusarium graminearum* virus-DK21, which is phylogenetically related to hypoviruses but has a genome organization and gene expression strategy resembling those of plant potex-like viruses. *Mol. Cells*, 28, 73-74.
- Lee, K.-M., Cho, W.-K., Yu, J., Son M., Choi. H., Min K., Lee Y.-W, and Kim K.-H. (2014) A comparison of transcriptional patterns and

- mycological phenotypes following Infection of *Fusarium graminearum* by Four mycoviruses. *PLoS One*, 9, e100989.
- Lee, K.-M., Yu, J., Son, M., Lee, Y.-W. and Kim, K.-H. (2011) Transmission of *Fusarium boothii* mycovirus via protoplast fusion causes hypovirulence in other phytopathogenic fungi. *PLoS One*, 6, e21629.
- Nuss, D. L., (2005) Hypovirulence: mycoviruses at the fungal–plant interface. *Nat. Rev. Microbiol.* 3, 632-642.
- Pearson, M. N., Beever, R. E., Boine, B. and Arthur, K. (2009) Mycoviruses of filamentous fungi and their relevance to plant pathology. *Mol. Plant Pathol.* 10, 115-128.
- Son, M., Lee, K.-M., Yu, J., Kang, M., Park, J. M., Kwon S.-J. and Kim, K.-H. (2013) The *HEX1* gene of *Fusarium graminearum* is required for fungal asexual reproduction and pathogenesis and for efficient viral RNA accumulation of *Fusarium graminearum* virus 1. *J. Virol.* 87, 10356-10367.
- Soundararajan, S., Jedd, G., Li, X., Ramos-Pamplona, M., Chua, N. H. and Naqvi, N. I. (2004) Woronin body function in *Magnaporthe grisea* is essential for efficient pathogenesis and for survival during nitrogen starvation stress. *Plant Cell*, 16, 1564-1574.

- Wang, R. and Li, K. (2012) Host factors in the replication of positive-strand RNA viruses. *J. Chang Gung Med.* 35.
- Yu, J., Kwon, S.-J., Lee, K.-M., Son, M. and Kim, K.-H. (2009) Complete nucleotide sequence of double-stranded RNA viruses from *Fusarium graminearum* strain DK3. *Arch. Virol.* 154, 1855-1858.
- Yu, J., Lee, K.-M., Son, M. and Kim, K.-H. (2011) Molecular characterization of *Fusarium graminearum* virus 2 Isolated from *Fusarium graminearum* strain 98-8-60. *J. Plant Pathol.* 27, 285-290.
- Yu, X., Li, B., Fu, Y., Jiang, D., Ghabrial, S. A., Li, G., Peng, Y., Xie, J., Cheng, J. and Huang, J. (2010) A geminivirus-related DNA mycovirus that confers hypovirulence to a plant pathogenic fungus. *Proc. Nat. Acad. Sci. USA*, 107, 8387-8392.
- Yuan, P., Jedd, G., Kumaran, D., Swaminathan, S., Shio, H., Hewitt, D., Chua, N. H. and Swaminathan, K. (2003) A HEX-1 crystal lattice required for Woronin body function in *Neurospora crassa*. *Nat. Struct. Mol. Biol.* 10, 264-270.

CHAPTER I

**The *HEX1* gene of *Fusarium graminearum* is required
for fungal asexual reproduction and pathogenesis and
for efficient viral RNA accumulation of
Fusarium graminearum virus 1**

ABSTRACT

The accumulation of viral RNA depends on many host cellular factors. The hexagonal peroxisome (Hex1) protein is a fungal protein that is highly expressed when the DK21 strain of *Fusarium graminearum* virus 1 (FgV1) infects its host, and Hex1 affects the accumulation of FgV1 RNA. The Hex1 protein is the major constituent of the Woronin body (WB), which is a peroxisome-derived electron-dense core organelle that seals the septal pore in response to hyphal wounding. To clarify the role of Hex1 and the WB in the relationship between FgV1 and *Fusarium graminearum*, targeted gene deletion and over-expression mutants were generated. Although neither *HEX1* gene deletion nor over-expression substantially affected vegetative growth, both changes reduced the production of asexual spores and reduced virulence on wheat spikelets in the absence of FgV1 infection. However, vegetative growth of deletion and over-expression mutants were increased and decreased, respectively, upon FgV1 infection compared to that of FgV1-infected wild-type isolate. Viral RNA accumulation was significantly decreased in deletion mutants but was significantly increased in over-expression mutants compared to the wild-type virus-infected control. Overall, these data indicate that the *HEX1* gene plays a direct role in the

asexual reproduction and virulence of *F. graminearum* and facilitates viral RNA accumulation in the FgV1-infected host fungus.

INTRODUCTION

The interactions between viral elements and host factors are important for maintaining the infection cycles of RNA viruses in host cells. Viruses utilize numerous host factors that play essential roles in virus infection. Therefore, understanding the role(s) of host factors can provide insight into the molecular mechanism(s) of host and virus interactions. Relative to host factors affecting RNA viruses of animals and plants, host factors affecting fungal viruses (mycoviruses) are poorly understood.

Several host and viral components required for the virus life in cells have been identified and characterized in the model organism, *Saccharomyces cerevisiae*. The knowledge obtained by studying *S. cerevisiae* as a host for several dsRNA and ssRNA viruses has greatly extended our understanding of mycovirus-host interaction (Wickner et al., 2013). With respect to filamentous fungi, host factors required for mycovirus replication and symptom induction have been well described for the interaction between the prototypic hypovirus *Cryphonectria hypovirus 1*-EP713 (CHV1) and its host, the chestnut blight fungus (*Cryphonectria parasitica*). One of these host factors, NAM-1, modulates symptom induction in the fungus in response to CHV1 infection (Faruk et al., 2008). The hypovirus-responsive

host transcription factor gene *pro1* is required for female fertility of *C. parasitica*, development of its asexual spores, and the maintenance of CHV1 infection (Sun et al., 2009). The host gene *Cpbir1*, which encodes the IAP (inhibitor of apoptosis protein) CpBir1 and which is required for fungal conidiation, virulence, and anti-apoptosis, is considerably down-regulated as a consequence of hypovirus infection and affects hypovirus transmission in *C. parasitica* (Gao et al., 2012). Although much has been learned about the functional roles of host factors in the interaction between CHV1 and *C. parasitica*, how host components affect replication and movement in other mycovirus–fungus systems is largely unknown.

The current paper concerns the interaction of a mycovirus with the plant-pathogenic fungus *Fusarium graminearum* Schwabe [Teleomorphs: *Gibberella zeae* (Schwein.) Petch]. *F. graminearum* is the causal agent of cereal head blight on crops such as maize, barley, and wheat (Lin et al., 2011, Min et al., 2010, Son et al., 2011a and 2011b). A number of mycoviruses have been reported to infect *F. graminearum* (Chu et al., 2002 and 2004, Darissa et al., 2011 and 2012, Kwon et al., 2009, Wang et al., 2013, Yu et al., 2009 and 2011), and some of these results in fungal hypovirulence (Aminian et al., 2011, Chu et al., 2002, Darissa et al., 2012, Wang et al., 2013). It is previously reported that the dsRNA mycovirus

Fusarium graminearum virus 1-strain DK21 (currently named FgV1), reduces the virulence of *F. graminearum* and also delays mycelial growth, increases pigmentation, and reduces the production of mycotoxin (Chu et al., 2002). To identify host factor(s) involved in FgV1–*F. graminearum* interactions, putative genes or gene products were screened based on transcriptional and proteomic analysis (Cho et al., 2012 and 2013, Kwon et al., 2009). Research on this mycovirus–fungus interaction will be facilitated by a well-developed DNA-mediated transformation system for *F. graminearum*, which enables efficient genetic alteration such as targeted gene deletion and over-expression of endogenous genes by promoter switching (Lin et al., 2011). Research on this mycovirus–fungus interaction will also be facilitated by the genome-wide functional analysis of transcription factors (Son et al., 2011b).

Recent report demonstrated that at least 22 proteins of *F. graminearum* are differentially expressed in response to FgV1 infection (Kwon et al., 2009). One of the highly expressed proteins is the peroxisome-derived hexagonal protein (Hex1) (locus FGSG_08737). The Hex1 protein self-assembles to form the Woronin body (WB). The WB is a peroxisome-derived dense-core microbody that is specific to filamentous ascomycetes (Jedd et al., 2000, Leal et al., 2009, Managadze et al., 2007, Ng

et al., 2009, Soundararajan et al., 2004, Tenney et al., 2000, Tey et al., 2005, Yuan et al., 2003). WBs maintain cellular integrity by sealing the septal pore after cellular damage in *Neurospora crassa* (Jedd et al., 2000). WBs are also involved in pathogenesis and survival under nitrogen-starvation conditions in *Magnapothae oryzae*; deletion of the *HEX1* gene causes appressorial defects and further reduces *M. oryzae* pathogenicity on barley and rice leaves (Soundararajan et al., 2004).

Here, I report that Hex1 functions in the maintenance of cellular integrity, the production of asexual spores, and the pathogenicity of *F. graminearum*. I also provide evidence that the *HEX1* gene acts as a host factor that enhances the accumulation of FgV1 RNA in *F. graminearum*. This is the first report concerning the effect of a host factor on the accumulation of a dsRNA mycovirus in an infected filamentous fungus.

MATERIALS AND METHODS

I. Fungal strains and culture conditions

All strains used in this study (Table 1) were stored in 25% (v/v) glycerol at -80°C and were reactivated on potato dextrose agar (PDA; Difco). For nucleic acid manipulation, all strains of *F. graminearum* were grown in 50 ml of a liquid complete medium [CM, (Lee et al., 2011)] at 25°C with shaking (150 rpm) for 5 days while strains of *C. parasitica* were grown in 50 ml of EP complete medium (Faruk et al., 2008) at 26°C with shaking (120 rpm) for 5 days. Mycelia were harvested by filtration through miracloth (Calbiochem) and ground to a fine powder with liquid nitrogen in a mortar and pestle.

II. Computational analysis

Nucleotide sequences from the NCBI database were assembled using the Seqman program in DNASTAR (<http://www.dnastar.com>). Sequence similarity searches of *HEX1* and *HEX1* homologs were conducted with the NCBI BLAST program. The alignment of Hex1 and Hex1 ortholog amino acid sequences was performed by the MegAlign program in DNASTAR, using a default setting and GeneDoc programs

(<http://www.nrbsc.org/gfx/genedoc/>). Phylogenetic analysis of amino acid sequences was inferred using the neighbor-joining method as previously described (Yu et al., 2009 and 2011). Evolutionary analysis was conducted in MEGA5 (<http://www.megasoftware.net>).

III. Genomic DNA extraction, primers, and PCR conditions

For extraction of genomic DNA, a previously described procedure were used (Lee et al., 2011). To construct a PCR fragment for deletion, over-expression, and complementation, a slightly modified double-joint (DJ) PCR strategy was applied for fusion of PCR products (Son et al., 2011a). The PCR construct for over-expression of the target gene was generated by same procedure that was used for the deletion mutants. The *gen* and elongation factor 1 promoter were amplified from the pSKGEN plasmid (Lin et al., 2011). For the complementation of deletion mutants, the hygromycin resistance gene cassette (*hph*) was amplified from the pBCATPH plasmid. General PCR was performed following the manufacturer's instructions (TaKaRa). The PCR primers used in this study (available upon request) were produced at an oligonucleotide synthesis facility (Bioneer).

IV. Fungal transformation for construction of targeted gene-deletion, over-expression, and complementation mutants

Protoplasts of the WT-VF strain (VF indicates virus free, VI indicates virus infected) were prepared by treating fresh mycelia grown in YPG liquid culture (0.3% yeast extract, 1% peptone, 2% glucose) for 3 h at 30°C with 1 M NH₄Cl containing 10 mg/ml of driselase (InterSpex Products) as previously described (Lee et al., 2011). Amplified PCR products were directly added with 1 ml of polyethylene glycol (PEG) solution (60% PEG 3350, 10 mM Tris-HCl pH 7.5, 10 mM CaCl₂) to protoplast suspensions as described above. Transformants with resistance to geneticin or hygromycin B were selected on regeneration medium containing 150 µg/ml of geneticin (Duchefa) or hygromycin B (Calbiochem). Selected transformants were infected by FgV1 using hyphal fusion-mediated virus transmission, and viral infection was confirmed by RT-PCR (described below). For the Southern blot hybridization of all mutants, the extracted genomic DNAs were digested with *Pst* I for 16 h at 37°C. A 10-µg quantity of digested DNA was separated on a 0.8% agarose gel for 8 h. The gels were capillary blotted onto positively charged nylon membranes (GE Healthcare) in 0.4 N NaOH for 12 h. The [³²P]-labeled DNA probes were generated following standard techniques as previously described (Lee et al., 2011). The hybridization

reaction was performed at 65°C for 16 h. After hybridization, unhybridized DNA probe was removed by washing with low (2x SSC and 0.1% SDS) and high (0.1x SSC and 0.1% SDS) stringency buffers. The blotting image was visualized using a Fuji BAS-2500 Phosphor Imager and corresponding imaging software (Fuji).

V. Radial growth, conidial production, and virulence test

Radial growth was measured on PDA, CM, and minimal medium (MM; 0.05% KCl, 0.2% NaNO₃, 3% sucrose, 1% KH₂PO₄, 0.05% MgSO₄·7H₂O, 0.02% trace element, 2% agar) at 5 days post-inoculation (dpi) as previously described (Lee et al., 2011).

To test the effect of *HEXI* deletion and over-expression on the virulence of *F. graminearum*, wheat head florets at early-mid anthesis were inoculated with conidial suspensions as described (Lee et al., 2011) on wheat cv. Jokyoung. Approximately 6-week-old wheat plants with flowering heads were used. For production of conidial inoculum, 10 mycelial plugs were incubated in CMC liquid medium (1.5% carboxymethyl cellulose, 0.1% yeast extract, 0.05% MgSO₄·7H₂O, 0.1% NH₄NO₃, and 0.1% KH₂PO₄) at 25°C with shaking (150 rpm) for 5 to 7 days. Conidia were collected by filtering through sterile miracloth. A 10-μl volume of the spore suspension

(10^5 conidia/ml) in 0.01% (v/v) Tween-20 was injected into one floret of each flowering wheat head. Wheat plants inoculated with 0.01% (v/v) Tween-20 alone served as a control. For each treatment, 10 replicate wheat heads were inoculated. Because the overexpression mutant produced no conidia when infected with FgV1 (see Results), the wheat heads were inoculated with 10 μ l of the CMC culture medium after that mutant had grown in the medium for 7 days. Inoculated plants were placed in a growth chamber (25°C, 80% relative humidity, 14/10 h light/dark cycle). The percentage of wheat heads with head blight symptoms was determined at 14 dpi. The test was repeated three times. Statistical analysis was performed using PASW statistics software (SPSS Inc.).

VI. Observation of WB formation using electron microscopy

Samples for transmission electron microscopy (TEM) were prepared as described previously (Kwon et al., 2009). All strains were grown on PDA plates at 25°C. Thin sections of mycelial agar plugs were used for preparing the samples. The ultrastructure of mycelia was observed with a transmission electron microscope (JEM 1010; JEOL).

VII. Measurement of intercalary length

For the measurement of intercalary length of hyphae (i.e., cell length of hyphae), sections of mycelia on the agar plates were microscopically examined as previously described (Wolkow et al., 1996). Differential interference contrast (DIC) images of conidia and hyphae were captured on a DE/Axio Imager A1 microscope (Carl Zeiss) with a CCD camera. The lengths of hyphal cells were measured using the AxioVision rel. 4.8 software program (Carl Zeiss).

For selecting mycelia at the same growth stage, I attempted to determine those parts of the colony that had undergone cytokinesis (the creation of septa) for a similar number of times. The average intercalary length (average hyphal cell size) of the strains were determined then identified the location of three growth stages by multiplying intercalary length by 0, 1000, and 2000. In other words, the initial inoculation point on the agar was established as “cytokinesis starting point 0” and the locations where cytokinesis had occurred 1000 and 2000 times were determined by multiplying the average intercalary length of the strain by 1000 or 2000. For example, when the intercalary length of WT-VI strain was 20.9 μm , then cytokinesis point 1000 and 2000 were determined to be located 2.09 cm and 4.18 cm away from “cytokinesis starting point 0”, respectively.

VIII. Fungal protein extraction and western blot analysis

For fungal protein extraction, the powdered mycelia were suspended with lysis buffer (Jedd et al., 2000). This lysate was filtered twice through miracloth, and the filtrate was centrifuged at 100×g for 5 min to remove unlysed cells. The lysate was then centrifuged at 10,000×g for 5 min, and the pellet was suspended in lysis buffer. A 200-μg quantity of total protein was resolved on a Mini-PROTEAN® TGX™ Precast gel (Bio-Rad) and transferred to a Hybond-P membrane (GE Healthcare) in transfer buffer (25mM Tris, 380 mM glycine, 20% methanol) at 100 V for 40 min for protein blot analysis. The membrane was blocked for 16 h in tris-buffered saline-Tween 20 (TBST) plus 2.5% skim milk (10 mM Tris pH 7.4, 100 mM NaCl, 0.05% (v/v) Tween-20). The membrane was then probed with anti-Hex1 antibody (1:200) in TBST plus 1% skim milk for 1 h at room temperature. The membrane was washed five times with TBST over the course of 1 h and probed with horseradish peroxidase-conjugated anti-rabbit IgG secondary antibody at 1:2000 dilution for 1 h. The membrane was then washed five times in TBST over the course of 1 h and evaluated for chemiluminescence using the Amersham ECL Western blotting detection reagents and analysis system (GE Healthcare) according to the manufacturer's protocol.

IX. RNA preparation and RT-PCR

For total RNA preparation, the powdered mycelia were suspended in Isol-RNA lysis reagent (5 PRIME). Nucleic acid was extracted by following the manufacturer's protocol with slight modification. The extracted total RNAs were purified twice with acid phenol:chloroform (1:1), precipitated with isopropanol, suspended in DEPC-treated water, and further treated with TURBO DNA-free™ (Ambion) to remove genomic DNA. The cDNAs were synthesized with M-MLV reverse transcriptase (Promega) and oligo d(T) primer to quantify *HEXI* mRNA expression and viral RNA accumulation. Quantitative real-time RT-PCR (qRT-PCR) was performed on a CFX96 Real-Time PCR System (Bio-Rad) using the SsoFast™ EvaGreen® Supermix (Bio-Rad) according to the manufacturer's instructions. After initial denaturation at 95°C for 10 min, 40 cycles consisted of 5 s at 95°C and 5 s at 58°C. Two endogenous reference genes, cyclophilin 1 (*CYP1*, locus FGSG_07439) and elongation factor 1 α (*EF1 α* , locus FGSG_08811), were used in each experiment. The endogenous reference gene for *C. parasitica*, glyceraldehyde-3-phosphate dehydrogenase (*GAPDH*) was used according to a previous report (Rostagno et al., 2009).

For the following experiment, all virus-infected strains were incubated in

square culture dishes (245×245×28 mm) (SPL LIFE SCIENCES) containing PDA. Mycelia were harvested from 1-cm² areas of the culture at cytokinesis point 0, 1000, and 2000, and were ground to a fine powder with liquid nitrogen in a mortar and pestle. Total RNAs and cDNAs for semi-quantitative RT-PCR (sqRT-PCR) were prepared using the same procedures described earlier. The sqRT-PCR was performed on a C1000™ Thermal Cycler (Bio-Rad). After initial denaturation at 95°C for 5 min, 35 or 40 cycles consisted of 30 s at 95°C, 30 s at 58°C, and 30 s at 72°C. Amplified DNA bands were analyzed by agarose gel electrophoresis.

Table 1. Fungal strains used in this study.

Strain	Description	Reference
WT-VF	Wild type (WT), virus-free; Lineage 3	Chu et al., 2002
WT-VI	WT-VF, infected with <i>Fusarium</i> <i>graminearum</i> virus 1 strain DK21 (FgV1)	Chu et al., 2002
$\Delta hex1$ -VF	<i>HEX1</i> deletion mutant in WT-VF genetic background	Son et al., 2013
$\Delta hex1$ -VI	$\Delta hex1$ -VF infected with FgV1	Son et al., 2013
<i>HEX1</i> OE-VF	<i>HEX1</i> over-expression mutant in WT-VF genetic background	Son et al., 2013
<i>HEX1</i> OE-VI	OE-VF infected with FgV1	Son et al., 2013
$\Delta hex1::HEX1$ -VF	Complemented with <i>HEX1</i>	Son et al., 2013
$\Delta hex1::HEX1$ -VI	$\Delta hex1::HEX1$ -VF infected with FgV1	Son et al., 2013
EP155	<i>Cryphonectria parasitica</i> mating type Mat-2	Lee et al., 2011
UEP	EP155 infected with CHV1	Lee et al., 2011
EP155-FgV1	EP155 infected with FgV1	Lee et al., 2011

RESULTS

I. Sequence analysis of *F. graminearum* *HEX1* and homologs from other plant-pathogenic fungi

The *F. graminearum* genomic DNA and mRNA of *HEX1* were sequenced using oligonucleotide primers specific for *HEX1* in PCR and RT-PCR. The 561-bp coding region contains a single 81-bp intron, which could encode a polypeptide with 186 amino acids and a molecular mass of about 20-kDa. The protein coding region was predicted according to previous reports of Hex1 (Jedd et al., 2000, Tenney et al., 2000, Soundararajan et al., 2004).

According to phylogenetic analysis using the putative amino acid sequence of *F. graminearum* Hex1 and homologs from other filamentous fungi, sequence identity with *F. graminearum* Hex1 was highest among *Fusarium* species including *F. oxysporum* and *F. verticillioides* (Fig. 1). Putative amino acid sequences of Hex1 homologs were more closely related among plant-pathogenic fungi than among animal-pathogenic fungi except in the case of *Chaetomium globosum*.

Computer-aided comparison of the deduced amino acid sequence of

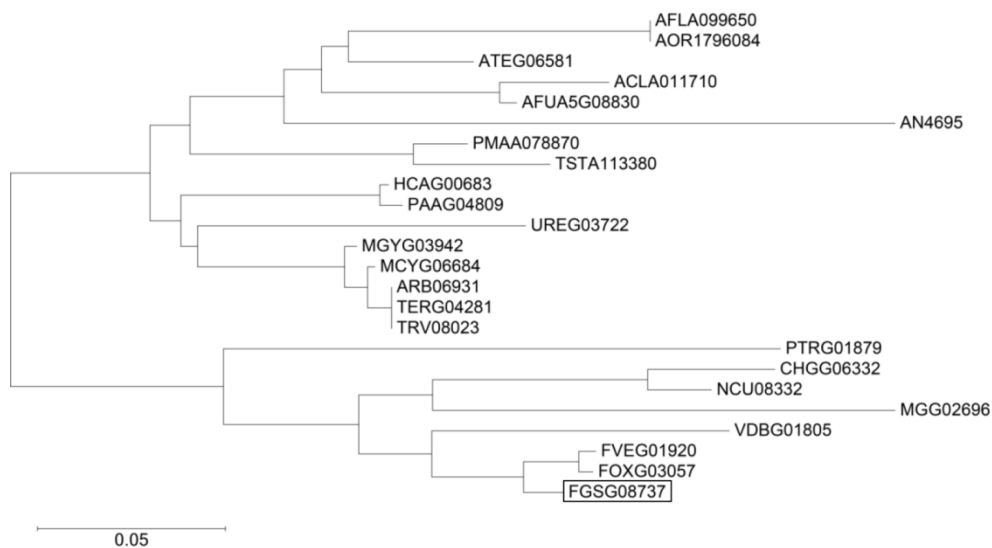


Fig. 1. Phylogenetic tree of predicted amino acid sequences of *HEX1* homologs. The tree was constructed by MEGA version 5.0 using the neighbor-joining method with default setting. The 0.05-scale bar represents 5% aberration. The amino acid sequences in this study are obtained from NCBI database.

β1 **H1** **β2**
 FgHEX1 : MGYDDDEG...SFRNGGIHLKLD...KS..REIEIDIRETSGPASS...PTGTSI CHHIRLGLIFL : 55
 FOXG03057 : MGYDDDDGHYNSFR.AGAHKLGDRIAHGGRRDIEIDIHEGPRPSADCLPNTVSI CHHIRLGLIFL : 64
 FVEG01920 : MGYDDDDGQYNSFR.AGAHKLGDRIAHGGRRDIEIDIHEGPRPSADCLLNTVSI CHHIRLGLIFL : 64
 MoHEX1 : MGYEDDR.....ETIEISESRVSRGSSRGPRSRGGDYAPTVSI CHHIRLGLIFL : 51
 NcHEX1 : MGYDDDD.....A...HG.HVEADAPRATTGTGTGSASCTVTI CHHIRLGLIFL : 46

β2 **β3** **β4** **β5** **β6** **β7**
 FgHEX1 : MLQGRPCQVIRISTSSATGQYRYLGVDLPTKQLHEESSFISNPAPSVVVC SMLGVEFKQYRVLDL : 120
 FOXG03057 : MLQGRPCQVIRISTSSATGQYRYLGVDLPTKQLHEESSFISNPAPSVVVC SMLGVEFKQYRVLDL : 129
 FVEG01920 : MLQGRPCQVIRISTSSATGQYRYLGVDLPTKQLHEESSFISNPAPSVVVC SMLGVEFKQYRVLDL : 129
 MoHEX1 : LLQGRPCQVIRISTSSATGQHRYLGVDLPTKELREESSISTPSPSVVVC TMCGFVEFKQYRVLDL : 116
 NcHEX1 : LLQGRPCQVIRISTSSATGQHRYLGVDLPTKQLHEESSFVSNPAPSVVVC TMLGVEFKQYRVLDL : 111

β8 **β9** **H2** **H3** **β10** **β10** **+++**
 FgHEX1 : QEGQIVAMTETGIVKQGLPVIDQSNLYSRLHNAFESGRGSVNVLVINDGGFELAVDMKVIHQSRRL : 185
 FOXG03057 : QEGQIVAMTETGIVKQGLPVIDQSNLYSRLSSAFESGRGSVNVLVINDGAFELAVDMKVIHQSRRL : 194
 FVEG01920 : QEGSIVAMTETGIVKQGLPVIDQSNLYSRLSSAFESGRGSVNVLVINDGAFELAVDMKVIHQSRRL : 194
 MoHEX1 : QAGHIVAMTETGIVKQNLVPVSEQSNLYERLQRAFESGRGSVNVLVINDGFEELVCDMAVLVHQSRRL : 181
 NcHEX1 : QDGSIVAMTETGIVKQNLVPVDSQSNLWNRLQRAFESGRGSVNVLVINDGHEGEMAVDMKVIHQSRRL : 176

Fig. 2. Deduced amino acid sequences alignment with closely related plant-pathogenic fungi. The alignment was conducted using MegAlign in Lasergene, using a default setting. FGSG_08737, *F. graminearum* Woronin body major protein; FOXG_03057, *F. oxysporum* hypothetical protein; FVEG_01920, *F. verticillioides* hypothetical protein; Nc_Hex1, *N. crassa* Hex1 protein; Mo_Hex1, *M. oryzae* Hex1 protein. The boxes indicate the structural motif of the Hex1 protein. For the letters above the boxes, H refers to the helix-turn-helix and β refers to the beta sheet. The location of the peroxisome targeting signal (S/R/L) is indicated by +++ above the box at the end of each sequence.

F. graminearum Hex1 showed high levels of sequence identity with Hex1 homologs from *F. oxysporum* (84%), *F. verticillioides* (82%), *N. crassa* (72%), and *M. oryzae* (67%) (Fig. 2). All predicted amino acid sequences of Hex1 and its homologs contained 14 motifs including 3 helix-turn-helix and 11 beta sheet motifs and peroxisome targeting sequences 1 (S/R/L). Given the high level of sequence identity, it can be designated locus FGSG_08737 as Hexagonal protein 1 gene (*HEX1*) in *F. graminearum*.

II. Targeted deletion, over-expression, and complementation of the *HEX1* gene

Targeted gene-deletion ($\Delta hex1$) and over-expression (*HEX1* OE) mutants were generated to examine the role(s) of the *HEX1* gene in the growth and pathogenicity of *F. graminearum* as well the effect of the gene on the accumulation of FgV1. *HEX1* was successfully replaced with *gen* by homologous recombination and complemented with *hph* construct (Fig. 3A, C). Hex1 over-expression mutants in which the *HEX1* gene is under the control of the *EF1 α* promoter ($P_{EF1\alpha}$) from *F. verticillioides* were also generated (Fig. 3B). All of the genetically manipulated strains were confirmed by Southern hybridization (Fig. 4).

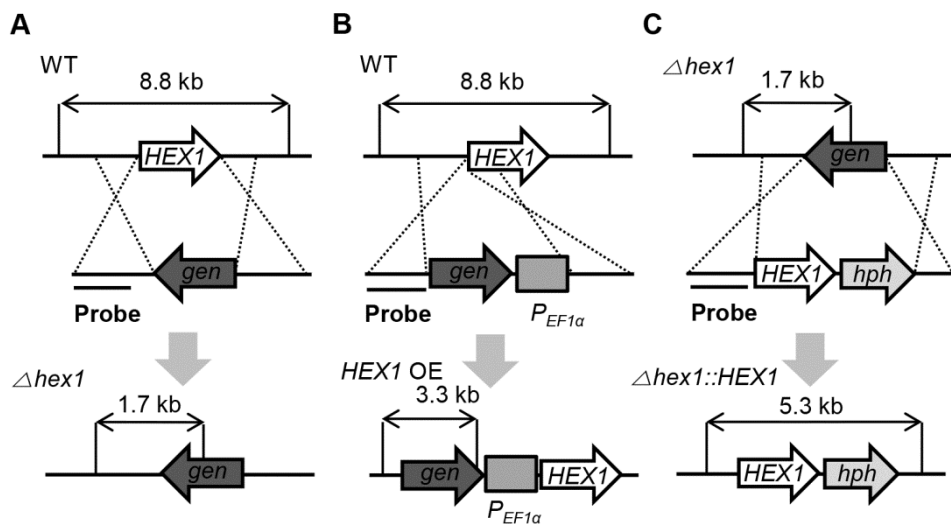


Fig. 3. Construction strategy of *HEX1* gene-deletion, over-expression, and complementation mutants in *F. graminearum*. (A) The *HEX1* ORF from the wild-type (WT) genome was replaced with the geneticin resistance gene cassette to construct $\Delta hex1$ mutants. (B) The geneticin resistance gene cassette and $P_{EF1\alpha}$ fragment were inserted into upstream of *HEX1* ORF to generate *HEX1* OE mutants. (C) The $\Delta hex1$ mutant was complemented by introducing *HEX1* ORF ($\Delta hex1::HEX1$) with the hygromycin B resistance gene cassette into the $\Delta hex1$ strain.

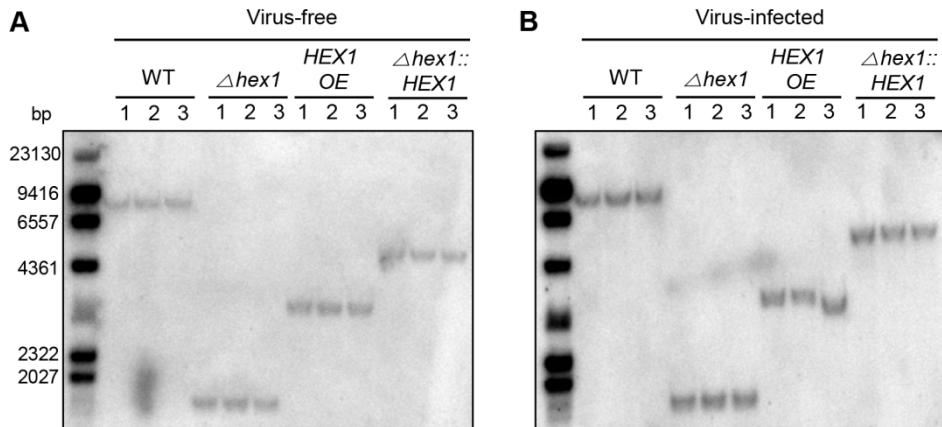


Fig. 4. Southern blot hybridization. *HEX1* mutants were confirmed by DNA gel blot analysis. When the 5' flanking region was used as a probe for southern blot hybridization, the genomic DNA digested with *Pst* I from the four genetically different strains generated distinguishable hybridized DNA fragments of 8.8 kb for the wild type, 1.7 kb for the $\Delta hex1$ mutant, 3.3 kb for the *HEX1* OE mutant, and 5.3 kb for the complemented mutant. All strains were constructed using a PCR-based strategy as described in the Materials and Methods.

Quantitative RT-PCR was performed to confirm the transcript level of deletion and over-expression mutants. The expression level of *HEX1* mRNA in the *HEX1* OE strain was up-regulated by about three times under the control of the *EF1 α* promoter (Fig. 13A). All of these *HEX1* gene mutants were without virus infection and are denoted as virus-free (VF). Virus-infected strains obtained by hyphal fusion-mediated transmission using a wild-type virus-infected strain of *F. graminearum* are denoted as virus-infected (VI). The genetic characteristics of all fungal strains used in this study are listed in Table 1.

III. Colony morphology and vegetative growth of *HEX1* mutants

On PDA at 5 dpi, the colony morphologies were very similar among WT-VF, $\Delta hex1$ -VF, *HEX1* OE-VF, and $\Delta hex1::HEX1$ -VF strains under standard laboratory conditions (Fig. 5, top row). All strains infected with FgV1 showed virus-associated phenotypic changes including reduced growth of aerial mycelia, increased pigmentation, and irregular colony morphology. However, there were distinguishable phenotypic characteristics among VI strains; among virus-infected strains, colony diameter was greatest for $\Delta hex1$ -VI, smallest for *HEX1* OE-VI, and intermediate for

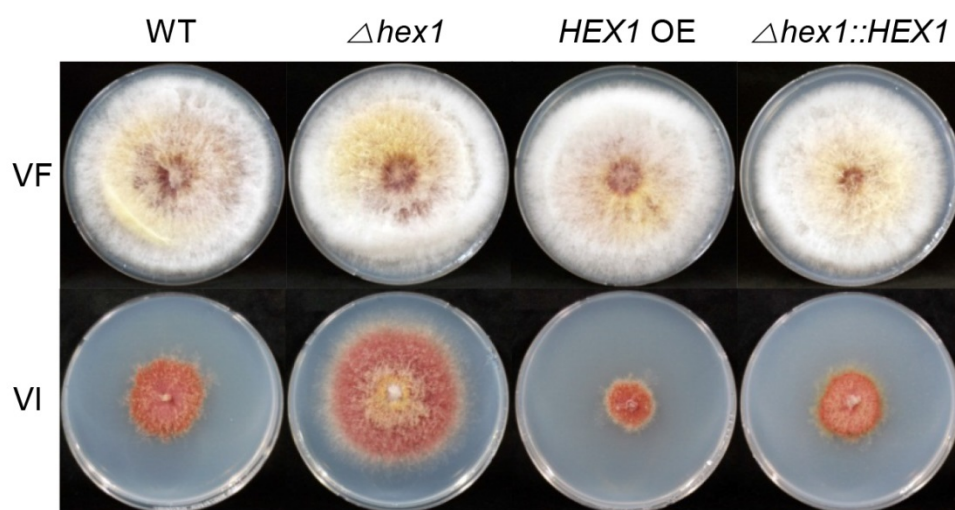


Fig. 5. Colony morphology of mutants. Colonies were photographed after 5 days on PDA

WT-VI and $\Delta hex1::HEX1$ -VI (Fig. 5, bottom row).

The radial growth on PDA, CM, and MM was measured to obtain quantitative data concerning vegetative growth. Among virus-free strains, radial growth on PDA was not significantly affected by gene deletion or over-expression (Fig. 6). Among virus-infected strains, radial growth was fastest for $\Delta hex1$ -VI, slowest for *HEX1* OE-VI, and intermediate for WT-VI and $\Delta hex1::HEX1$ -VI. Consistent with colony morphology, radial growth on PDA was slowest for *HEX1* OE-VI (Fig. 6). Results were similar on CM and MM (data not shown).

IV. Conidial production

Among virus-free strains, conidial production was significantly lower for $\Delta hex1$ -VF and *HEX1* OE-VF than for WT-VF and $\Delta hex1::HEX1$ -VF (Fig. 7). Relative to conidial production by WT-VF, conidial production was reduced for all four virus-infected strains. Among virus-infected strains, conidial production was about three-fold lower for $\Delta hex1$ -VI than for WT-VI, and *HEX1* OE-VI did not produce any conidia in CMC liquid medium. (Fig. 7).

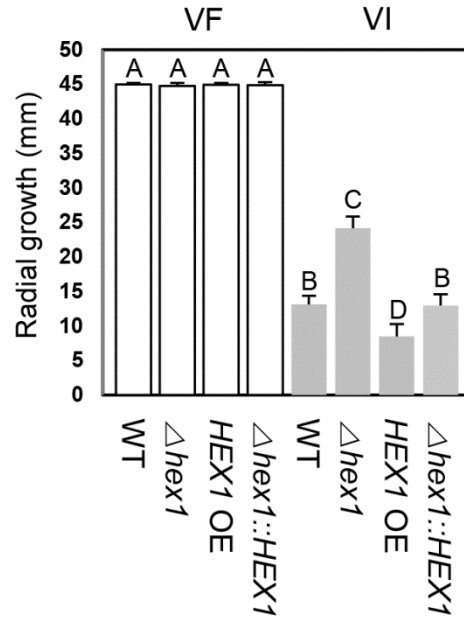


Fig. 6. Radial growth after 5 days on PDA. Error bars indicate the standard deviation, and values with different letters are significantly different at $p < 0.05$ based on the Tukey test.

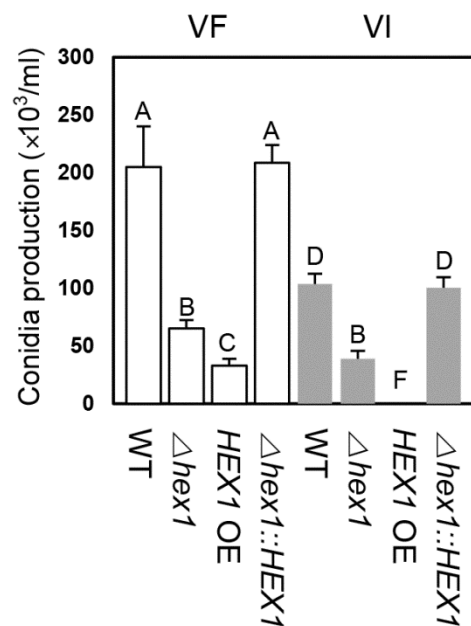


Fig. 7. Conidial production after 5 days in CMC liquid medium. Error bars indicate the standard deviation, and values with different letters are significantly different at $p < 0.05$ based on the Tukey test.

V. Subcellular localization of WBs and western blot analysis

TEM indicated that WBs were localized near septa but were absent in deletion mutants (Fig. 8). More WBs were detected in WT-VI than in WT-VF. WBs formed in *HEX1* OE strains and $\Delta hex1::HEX1$ strains with and without virus infection. In general, more WBs were observed in FgV1-infected than in VF strains of *HEX1* OE and $\Delta hex1::HEX1$.

Western blot analysis was carried out to verify genetic alteration and to support microscopic observation at the protein level using anti-*HEX1* antibody. One major band with a molecular mass of approximately 20 kDa was detected in all strains except the deletion mutants ($\Delta hex1$ -VF and $\Delta hex1$ -VI) and with slightly increased accumulation in WT-VI and $\Delta hex1::HEX1$ -VI (Fig. 9).

VI. Functions of the *HEX1* gene with respect to the maintenance of cellular integrity and pathogenesis

According to a previous report, deletion of the *HEX1* gene reduces the ability of *N. crassa* to maintain cellular integrity (Jedd et al., 2000). To determine whether the *HEX1* gene has a similar role in *F. graminearum*, we

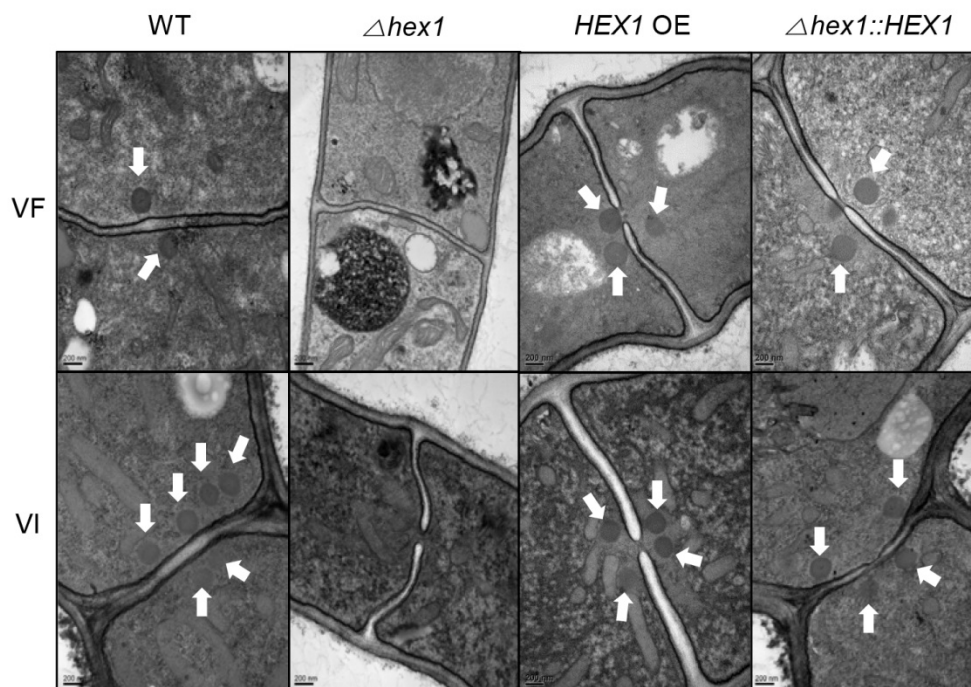


Fig. 8. Subcellular localization of Woronin bodies (WBs). White arrows near the septa point to WBs. As indicated, bars = 200 nm or 0.5 μ m. The sections were photographed with a transmission electron microscope (JEM 1010; JEOL).

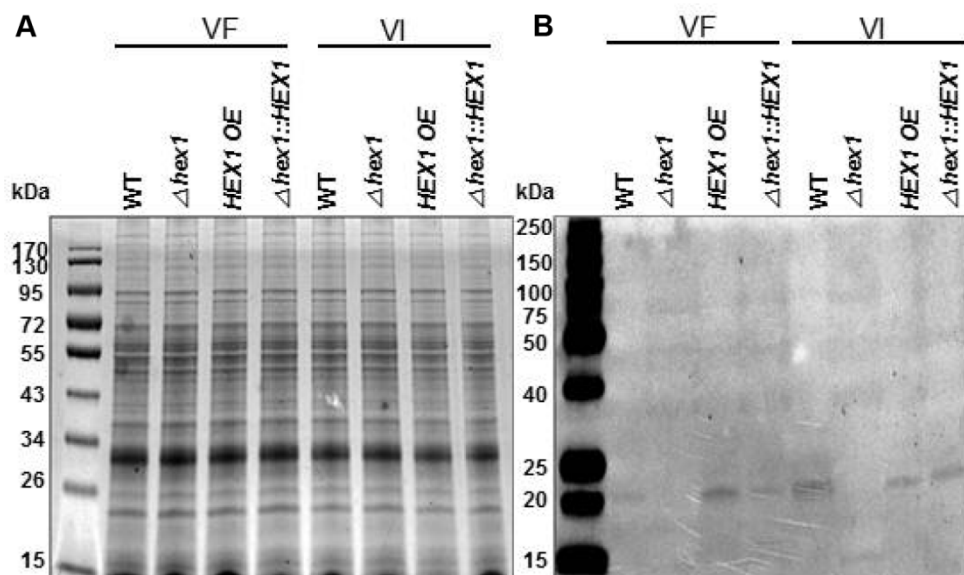


Fig. 9. Western blot analysis using Hex1 antibody in the *HEX1* mutants. (A) SDS-PAGE gel analysis of fungal total protein from all strains. The samples were analyzed in 12% polyacrylamide containing gel and further stained using coomassie blue. (B) Western blot analysis using Hex1 antibody. Fungal total proteins were loaded on a 12% SDS-PAGE gel. Protein gel blot analysis of the respective lysates was conducted using antibody against the Hex1 of *N. crassa* to detect the *F. graminearum* homologs.

used light microscopy to observe the growth rate of mycelia after the mycelia were wounded by amputation. The mycelial growth after amputation was delayed when the *HEX1* gene was deleted. Six hours after amputation, the quantity of new growth was much less in $\Delta hex1$ -VF than in WT-VF, *HEX1* OE-VF, or $\Delta hex1::HEX1$ -VF (Fig. 10). Cytoplasmic bleeding in all virus-free strains was assessed according to previous reports (Soundararajan et al., 2004, Tenney et al., 2000). Cytoplasmic bleeding was observed only in $\Delta hex1$ -VF strain at 3 hpi in a cutting plane and peripheral area of the cutting plane (Fig. 11).

In the pathogenicity test, deletion of *HEX1* among the virus-free strains significantly reduced head blight symptoms (Fig. 12A and B). Surprisingly, over-expression of *HEX1* also reduced head blight symptoms. Head blight symptoms were less severe on virus-infected than on virus-free strains. *HEX1* OE-VI, which produced no conidia (Fig. 7), did not induce any symptoms when wheat heads were inoculated with its culture filtrate..

VII. Quantification of *HEX1* gene expression

qRT-PCR was conducted to measure the expression level of *HEX1* and its homologs in the parental strain and in the other plant-pathogenic

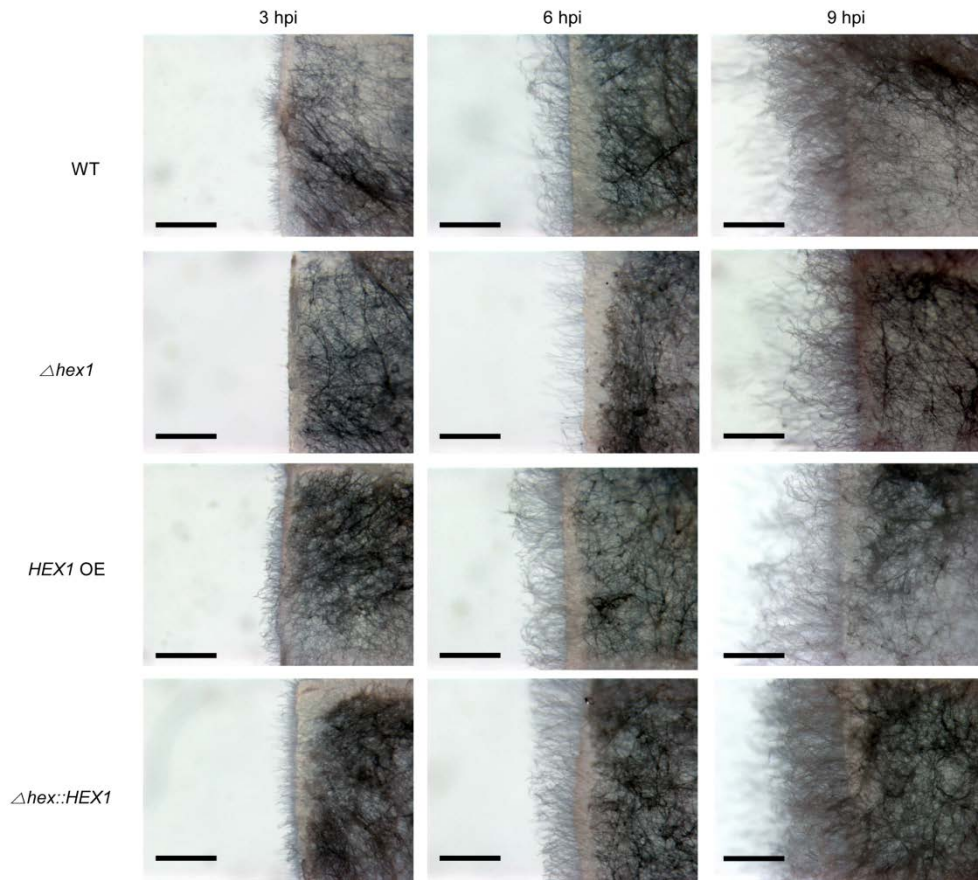


Fig. 10. Growth of hyphae of WT-VF, $\Delta hex1$ -VF, *HEX* OE-VF, and $\Delta hex1::HEX1$ -VF strains after amputation with a razor blade. The strains were growing on PDA, and the amputated and re-growing hyphae, which were located on the colony margin, were photographed at 3, 6, and 9 h after amputation. Bars indicate 1000 μ m.

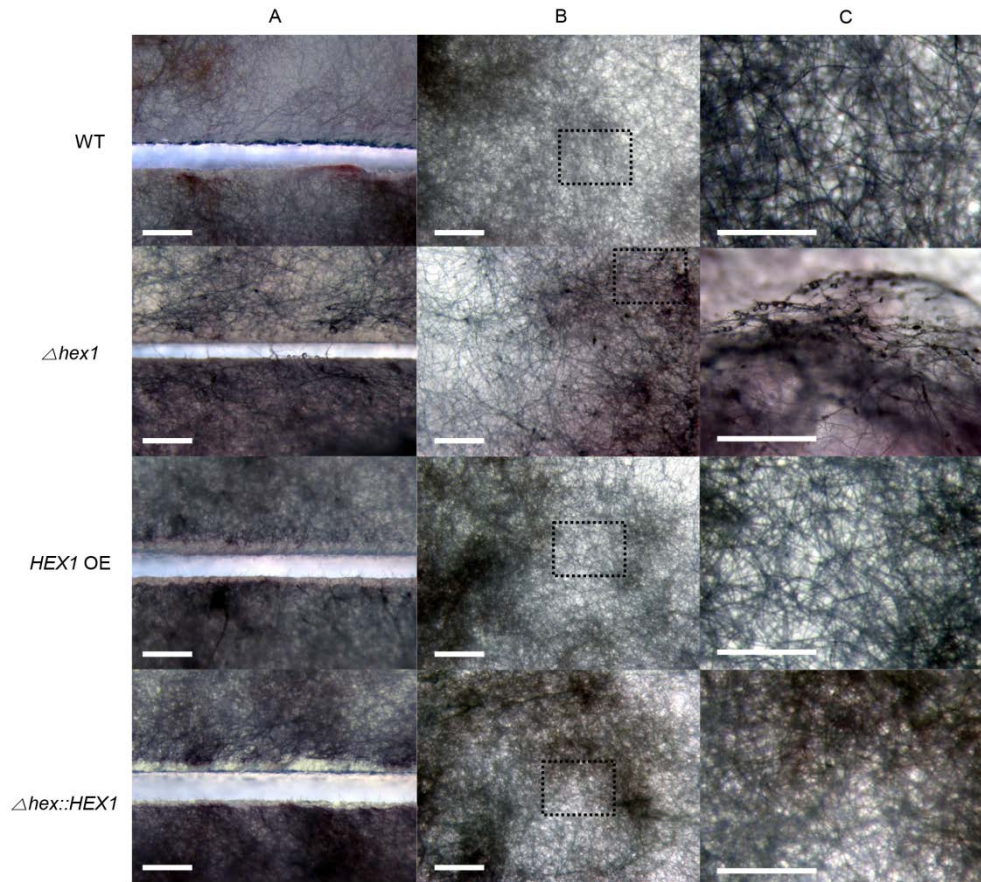


Fig. 11. Cytoplasmic bleeding in the *HEX1* deletion strain. Photographs of WT-VF, $\Delta hex1$ -VF, *HEX* OE-VF, and $\Delta hex1::HEX1$ -VF strains after amputation with a razor blade. The strains were growing on MM, and the amputated and re-growing hyphae, which were located on cutting planes and the peripheral area of the cutting planes, were photographed at 3 h after amputation. Panels A-C indicate the area where photographs were taken i.e. A for the cutting plane, B for the peripheral zone of the cutting plane, and C for the magnified images from dotted boxes in B, respectively. Bars indicate 500 μ m.

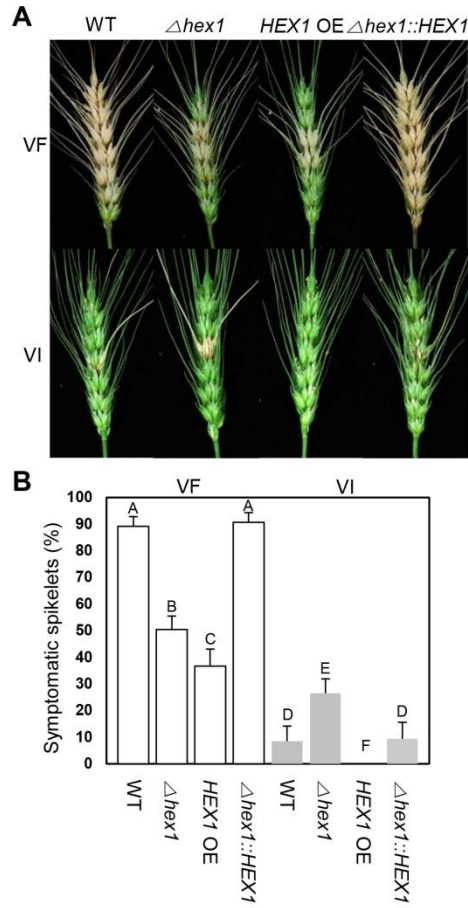


Fig. 12. Virulence assay with $HEX1$ mutants and the wild type (WT) of *F. graminearum* that were infected with FgV1 (indicated by VI) or virus free (indicated by VF). (A) Disease symptoms in wheat head spikelets. Conidial suspensions of the three mutants and the WT were used to inoculate wheat plants, except that culture filtrate was used for $HEX1$ OE-VI because that mutant did not produce conidia when infected with FgV1. The culture filtrate inoculum of $HEX1$ OE-VI was treated in the same manner as the conidial inoculums of the other strains. The wheat heads were photographed at 14 dpi. (B) Disease severity was evaluated at 14 dpi. Error bars indicate standard deviation. Values with different letters are significantly different at $p < 0.05$ based on the Tukey test

fungus (*C. parasitica*). The references and sources of VF and VI strains of these isolates were described previously (Lee et al., 2011, Table 1). The qRT-PCR analysis revealed that *HEX1* expression level was more than 6-fold greater in WT-VI than in WT-VF at 5 dpi (Fig. 13A). Relative to expression in WT-VF, the expression level was increased by approximately 3.5-fold in *HEX1* OE-VF and by more than 5-fold in *HEX1* OE-VI (Fig. 13A). The *HEX1* transcript was not detected in either of the *HEX1* deletion mutants. In *C. parasitica*, expression of the *HEX1* homolog was much greater with virus infection than without and was much greater with FgV1 infection than with CHV1 infection (Fig. 13B).

VIII. Quantification of FgV1 viral RNA accumulation

qRT-PCR was used to measure the accumulation of FgV1 RNA in the four *F. graminearum* strains that were infected with the virus. FgV1 RNA accumulation was substantially lower in the *HEX1* deletion mutant than in the WT but was similar in the complemented mutant and the WT (Fig. 14). FgV1 RNA accumulation was much greater in the overexpression mutant than in the other strains (Fig. 14).

Semi-quantitative (sq) RT-PCR was also conducted to verify FgV1 accumulation based on the number of times of cytokinesis had occurred

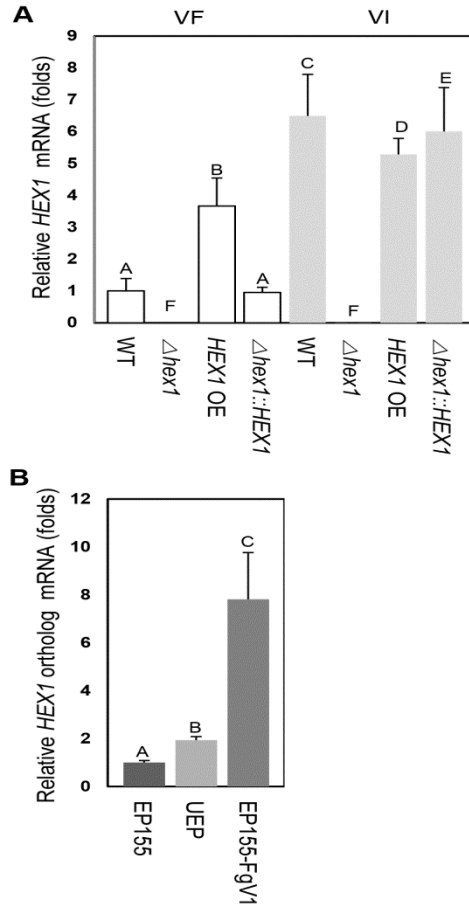


Fig. 13. qRT-PCR analysis of expression of *HEX1* and its orthologs in *F. graminearum* and *Cryphonectria parasitica* as affected by mycovirus infection. (A) Relative *HEX1* mRNA expression in the WT-VF, WT-VI, $\Delta hex1$ -VF, $\Delta hex1$ -VI, *HEX1* OE-VF, *HEX1* OE-VI, $\Delta hex1::HEX1$ -VF, and $\Delta hex1::HEX1$ -VI strains of *F. graminearum*. Relative transcript levels were normalized using cDNA of elongation factor 1 α and cyclophilin 1. (B) Relative mRNA expression of *HEX1* homologs in *C. parasitica*. EP155 refers to virus-free *C. parasitica* mating type Mat-2; UEP refers to EP155 infected with CHV1; and EP155-FgV1 refers to EP155 infected with FgV1. In (A) and (B), error bars indicate standard deviation. Values with different letters are significantly different at $p < 0.05$ based on the Tukey test.

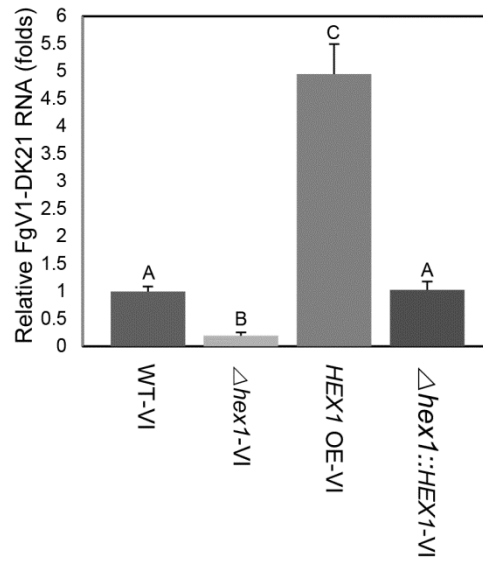


Fig. 14. Quantification of FgV1 viral RNA accumulation in *F. graminearum* using qRT-PCR. Relative accumulation of FgV1 viral RNA in WT-VI, $\Delta hex1$ -VI, OE-VI, and $\Delta hex1::HEX1$ -VI strains. Error bars indicate standard deviation. Values with different letters are significantly different at $p < 0.05$ based on the Tukey test.

(i.e., based on growth stage) in growing mycelia of all infected strains (see Materials and Methods; Table 2). The intensities of amplified DNA bands using the FgV1-specific primer set were verified in same manner as in the qRT-PCR analysis. Viral RNA accumulation was decreased in $\Delta hex1$ -VI, recovered in $\Delta hex1::HEX1$ -VI, and increased in *HEX1* OE-VI. All amplified DNA fragments showed different intensities based on the number of times cytokinesis had occurred. As the number of times cytokinesis occurred increased, the intensities diminished in all four kinds of VI strains (Fig. 15).

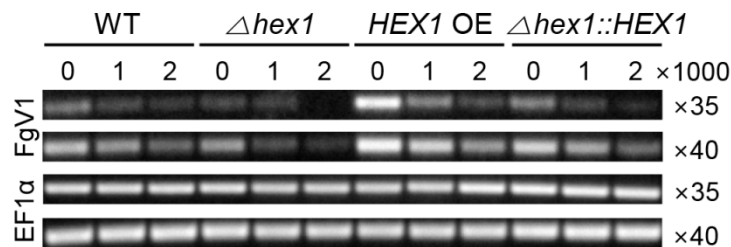


Fig. 15. Quantification of FgV1 viral RNA accumulation in *F. graminearum* using sqRT-PCR. Semi-quantitative RT-PCR using FgV1-specific primers. Total RNAs for reverse transcription were extracted from PDA plates based on the number of cytokinesis events, i.e., based on the growth stage of the strain. Amplified DNAs using the *EF1α* gene-specific primer set were loaded as a control (lower panel). Numbers on the right side of the ethidium bromide stained gel image indicate the number of cytokinesis events (×1000 and ×2000) and the number of PCR cycles (×35 and ×40).

Table 2. Average intercalary lengths (= cell length) of the *HEX1* mutants and the wild type (WT) of *F. graminearum* that were infected with FgV1 (indicated by VI) or virus free (indicated by VF)^a. ^a The fungi were growing on solid agar medium (PDA). Values within a column with different letters are significantly different ($p<0.05$) based on the Tukey test

Strain	Intercalary length (μm)
WT-VF	38.3 ^A
WT-VI	20.9 ^C
$\Delta hex1$ -VF	32.6 ^B
$\Delta hex1$ -VI	18.7 ^C
<i>HEX1</i> OE-VF	37.6 ^A
<i>HEX1</i> OE-VI	12.1 ^D
$\Delta hex1::HEX1$ -VF	37.8 ^A
$\Delta hex1::HEX1$ -VI	19.9 ^C

DISCUSSION

In this study, I characterized the *F. graminearum* *HEX1* gene, which encodes a protein that forms Woronin bodies (WBs) in filamentous fungi. The $\Delta hex1$ strain of *F. graminearum* did not form these cellular organelles, and although its colony morphology was normal, the $\Delta hex1$ strain exhibited reduced radial growth after injury, indicating that WBs play an important role in maintaining cellular integrity. Our observations of the $\Delta hex1$ strain also confirmed that WBs are important for fungal virulence. Although these functions of WBs have been reported for other fungi (Jedd et al., 2000, Tenney et al., 2000, Yuan et al., 2003), it is noteworthy that WBs also have the same functions in *F. graminearum*, which is an important plant-pathogen.

According to the *Fusarium* comparative database of the Broad Institute (http://www.broadinstitute.org/annotation/genome/fusarium_group), the coding region of the *FGSG_08737* gene (designated as *HEX1* in this study) consists of 1859 bp, and the predicted protein has 514 amino acids and a molecular mass of about 74 kDa. The results of our sequence analysis and western blot analysis indicated a coding region of 561 bp and a 20-kDa

protein. Even though our western blot analysis used antibody that can cover sequences upstream of the 561 bp coding region, I could not detect any specific protein bands corresponding to the 74-kDa protein band in repeated experiments (data not shown). Previous western blot analyses using the same antibody from *N. crassa* and *M. oryzae* also demonstrated that the molecular mass of the protein encoded by the *HEX1* gene is about 20 kDa (Jedd et al., 2000, Soundararajan et al., 2004). Moreover, analyses based on nucleic acid and amino acid sequences and on the function of the Hex1 protein in previous studies and in the present study strongly suggest that Hex1 shares both sequence and functional homologies among filamentous fungi. I therefore conclude that the molecular mass of the protein encoded by the *HEX1* gene is 20 kDa in *F. graminearum*, as it is in other filamentous fungi.

In accordance with a previous proteomic study (Kwon et al., 2009), An incubation period of 5 days was used for all fungal strains except in the production of conidia for the virulence assay. I first measured conidial production of strains at 5 dpi (Fig. 7), and then extended incubation for 2 days to collect more conidia from both deletion and over-expression mutants. Surprisingly, the rate of sporulation for the virus-infected strains was reduced by about half relative to our previous study (Chu et al., 2002). This

difference between the two studies might result from differences in the fungal host strain, the amount of initial inoculum, or the incubation time in CMC medium. The difference might also result from an unknown alteration of the fungal host or mycovirus during successive serial culturing after isolation.

The virulence test with wheat plants showed that deletion of the *HEX1* gene reduced *F. graminearum* virulence by about 50%. This indicates that WBs are important to *F. graminearum* pathogenesis, which is in agreement with a previous study with *M. oryzae* (Soundararajan et al., 2004). While deletion of the *HEX1* gene did not affect conidia production by *M. oryzae*, it reduced conidia production by *F. graminearum* (Fig. 7). In the case of *M. oryzae*, deletion of *HEX1* resulted in severe morphological defects in appressoria and a delay in host penetration (Soundararajan et al., 2004), and such abnormalities evidently explained the diminished virulence for the *HEX1* gene deletion mutant of *M. oryzae*. Overall, the reduced virulence of *HEX1* deletion mutants in both *F. graminearum* and *M. oryzae* seems to be caused by reduced viability of conidia.

Like the deletion mutant, the *HEX1* OE mutant exhibited reduced conidia production and virulence while showing normal vegetative growth (Fig. 5, 6, 7 and 12). The results obtained with the *HEX1* OE mutant might be

explained by the constitutive expression of *HEX1* by $P_{EF1\alpha}$. In other words, abnormal over-expression of *HEX1* might explain the defects in asexual reproduction and conidia viability during pathogenesis. In this regard, the WT-VI strain, which had the highest expression level of *Hex1* among all strains, also showed reduced conidial production and virulence. Also, more FgV1 viral RNA accumulated in the *HEX1* OE-VI mutant than in any of the other virus-infected strains even though *HEX1* expression in the other virus-infected strains (except the virus-infected deletion strain) was equivalent to that in the *HEX1* OE-VI mutant (Fig. 13A, Fig. 14). This result might also be explained by the constitutive expression of *HEX1* by $P_{EF1\alpha}$. In other words, continuous production of *HEX1* seemed to facilitate the constant accumulation of FgV1 viral RNA. Taken together, these results suggest that a moderate level of *HEX1* gene expression might be required for normal asexual reproduction and pathogenesis by *F. graminearum* and for FgV1 viral RNA accumulation in *F. graminearum*.

Semi-quantitative RT-PCR was conducted to investigate the cause of colony morphological differences among VI strains. To sample mycelia at similar growth stages, I harvested growing mycelia on PDA according to the number of times the cells had undergone cytokinesis rather than according to a set location of the growing hyphae. In agreement with the qRT-PCR

results, accumulation of FgV1 viral RNA in a solid culture medium depended on the genetic alteration of *HEX1* (Fig. 14 and 15). In conclusion, the relative accumulation of viral RNA among the VI strains (the virus-infected strains) was inversely related to their colony growth. Estimating the number of times cells had undergone cytokinesis by measuring intercalary lengths (cell size) of all strains provided additional evidence that the deletion of *HEX1* and FgV1 infection decreased cell size (Table 2). However, a moderate decrease of cell size in the $\Delta hex1$ -VF strain among VF strains may not affect vegetative growth. In contrast, FgV1 infection severely decreased cell size in all VI strains. This result suggested that the severe decrease of cell size by FgV1 infection resulted in reduced growth of the fungal host.

Many mycoviruses have been identified and characterized from various filamentous fungi (Ghabrial and Suzuki., 2009, Pearson et al., 2009) but only a few confer hypovirulence to their fungal host, and these include *Botrytis cinerea* debilitation-related virus (BcDRV) (Wu et al., 2007), *Sclerotinia sclerotiorum* debilitation-associated RNA virus (SsDRV) (Xie et al., 2006), *Sclerotinia sclerotiorum* hypovirulence-associated DNA virus 1 (SsHADV-1) (Yu et al., 2010), and *Rosellinia necatrix* megabirnavirus 1 (RnMBV1) (Chiba et al., 2009). Although these are valuable resources for

studying hypovirulence caused by mycoviruses, CHV1 in *C. parasitica* remains a well-studied model system for understanding mycovirus-fungal host interactions (Allen et al., 2004, Deng et al., 2007, Suzuki et al., 2000).

Using genome-wide expression profiling analysis, it is reported recently that FgV1 causes transcriptional reprogramming of *F. graminearum* (Cho et al., 2012). Although the transcriptional expression profile of many host genes were significantly altered by FgV1 infection, it is difficult to determine whether these transcriptional changes also represent translational changes. At the start of our study, our hypotheses was that the up-regulation in *HEX1* transcription that occurs with FgV1 infection might be a cellular response to virus infection. This hypothesis was based on previous reports indicating that Hex1 and WBs function in the sealing of the septal pore after hyphal wounding (Tenney et al., 2000). However, both qRT-PCR and semi-quantitative RT-PCR demonstrated that the accumulation of FgV1 viral RNA decreased in deletion mutants and increased in over-expression mutants relative to the WT-VI strain (Fig. 14 and 15). The greater viral RNA accumulation in over-expression mutants than in deletion mutants strongly suggests that FgV1 accumulation depends on *HEX1* gene expression. The combined results suggest that Hex1 not only affects the formation of WBs (and therefore the sealing of septal pores) but also acts as a host factor that

increases the accumulation of FgV1 viral RNA.

Although the present study demonstrates that a single gene influences virus accumulation in a fungal host, the underlying molecular mechanism remains unknown. I speculate that *HEX1* functions as a host factor affecting cell-to-cell movement of FgV1 or replication of viral RNA for two reasons. First, Hex1 proteins self-assemble to form WBs as indicated earlier (Jedd et al., 2000). This process is promoted by the Woronin body Sorting Complex (WSC). The WSC is required to recruit Hex1 assemblies to the matrix face of the peroxisome membrane where they can bud off to produce the WB organelle (Liu et al., 2008). The WSC can also trigger cortical association (enveloping) of the WB, which allows partitioning of the nascent WB and segregation of the newly formed organelle into a subapical compartment. After WB biogenesis in the peroxisome membrane, the newly formed WB should be moved near a septal pore if it is to contribute to septal-pore sealing. In this relocation of the organelle, the *Leashin* (*Lah*) gene product is responsible for WB tethering (Ng et al., 2009). It is also well known that some plant virus use peroxisomes for their viral replication (McCartney et al., 2005). Especially in the case of *Tomato bushy stunt virus* (TBSV), viral RNA replication occurs on the surface of the cytosolic membrane of peroxisomes in plants and in yeast (Pathak et al., 2008). Based on the

previous reports concerning WB biogenesis (Jedd et al., 2000, Liu et al., 2008, Ng et al., 2000) and RNA viral replication on peroxisomes and on the current results concerning the presence of gene homologs related to WB biogenesis in *F. graminearum* (WSC for locus FGSG_01049 and Lah for locus FGSG_04119, respectively), it is tempting to speculate that FgV1 or other potential mycoviruses might use this tethering process to facilitate accumulation and intracellular movement of viral RNAs.

A second reason for suspecting that *HEX1* functions as a host factor affecting cell-to-cell movement of FgV1 or replication of viral RNA is that a previous report demonstrated that Hex1 protein shares sequence homology with eukaryotic translational initiation factor 5A (eIF-5A) (protein secondary structures designated Fig. 2; Yuan et al., 2003). The latter study also used X-ray diffraction crystallography to reveal that the tertiary structure of Hex1 is similar to that of eIF-5A in *N. crassa*. As a result of substantial research, the cellular functions of eIF-5A are now well known. It is interesting that eIF-5A binds to mRNA for translation elongation (Xu et al., 2004). Hence, I speculate that Hex1 might bind to FgV1 viral RNA and thereby enhance viral RNA replication.

Future research should focus on understanding how individual Hex1 proteins and/or WBs affect accumulation of FgV1 viral RNA. Research is

also needed to understand the molecular mechanisms of cell-to-cell movement and virus RNA replication.

LITERATURE CITED

- Allen, T. D. and Nuss D. L., (2004) Specific and common alterations in host gene transcript accumulation following infection of the chestnut blight fungus by mild and severe hypoviruses. *J. Virol.* 78, 4145-4155.
- Aminian, P., Azizollah, A., Abbas, S. and Naser, S. (2011) Effect of double-stranded RNAs on virulence and deoxynivalenol production of *Fusarium graminearum* isolates. *J. Plant Protec. Res.* 51, 29-37.
- Chiba, S., Salaipeth, L., Lin, Y. H., Sasaki, A., Kanematsu, S. and Suzuki, N. (2009) A novel bipartite double-stranded RNA mycovirus from the white root rot fungus *Rosellinia necatrix*: molecular and biological characterization, taxonomic considerations, and potential for biological control. *J. Virol.* 83, 12801-12812.
- Cho, W.-K., Yu, J., Lee, K.-M., Son, M., Min, K., Lee, Y.-W. and Kim, K.-H. (2012) Genome-wide expression profiling shows transcriptional reprogramming in *Fusarium graminearum* by *Fusarium graminearum* virus 1-DK21 infection. *BMC Genomics*, 13, 173.
- Cho, W.-K., Lee, K.-M., Yu, J., Son, M. and Kim, K.-H. (2013) Insight into

- mycoviruses infecting *Fusarium* species. *Adv. Virus Res.* 86, 273-288.
- Chu, Y.-M., Jeon, J.-J., Yea, S.-J., Kim, Y.-H., Yun, S.-H., Lee, Y.-W. and Kim, K.-H. (2002) Double-stranded RNA mycovirus from *Fusarium graminearum*. *Appl. Environ. Microbiol.* 68, 2529-2534.
- Chu, Y.-M., Lim, W.-S., Yea, S.-J., Cho, J.-D., Lee, Y.-W. and Kim, K.-H. (2004) Complexity of dsRNA mycovirus isolated from *Fusarium graminearum*. *Virus Genes*, 28, 135-143.
- Darissa, O., Willingmann, P., Schäfer, W. and Adam, G. (2011) A novel double-stranded RNA mycovirus from *Fusarium graminearum*: nucleic acid sequence and genomic structure. *Arch. Virol.* 156, 647-658.
- Darissa, O., Adam, G. and Schäfer, W. (2012) A dsRNA mycovirus causes hypovirulence of *Fusarium graminearum* to wheat and maize. *Eur. J. Plant Pathol.* 134, 181-189.
- Deng, F., Allen, T. D., Hillman, B. I. and Nuss, D. L., (2007) Comparative analysis of alterations in host phenotype and transcript accumulation following hypovirus and mycoreovirus infections of the chestnut blight fungus *Cryphonectria parasitica*. *Eukaryot. Cell*, 6, 1286-1298.

- Escaño, C. S., Juvvadi, P. R., Jin, F. J., Takahashi, T., Koyama, Y., Yamashita, S., Maruyama, J.-I. and Kitamoto, K. (2009) Disruption of the *Aopex11-1* gene involved in peroxisome proliferation leads to impaired woronin body formation in *Aspergillus oryzae*. *Eukaryot. Cell*, 8, 296-305.
- Faruk, M. I., Eusebio-Cope, A. and Suzuki, N. (2008) A host factor involved in hypovirus symptom expression in the chestnut blight fungus, *Cryphonectria parasitica*. *J. Virol.* 82, 740-754.
- Gao, K., Xiong, Q., Xu, J., Wang, K. and Wang, K. (2012) CpBir1 is required for conidiation, virulence and anti-apoptotic effects and influences hypovirus transmission in *Cryphonectria parasitica*. *Fungal Genet. Biol.* 51, 60-71.
- Ghabrial, S. A. and Suzuki, N. (2009) Viruses of plant pathogenic fungi. *Annu. Rev. Phytopathol.* 47, 353-384.
- Jedd, G. and Chua, N. H. (2000) A new self-assembled peroxisomal vesicle required for efficient resealing of the plasma membrane. *Nat. Cell Biol.* 2, 226-231.
- Kwon, S.-J., Lim, W.-S., Park, S.-H., Park, M.-R. and Kim, K.-H. (2009) Molecular characterization of a dsRNA mycovirus, *Fusarium graminearum* virus-DK21, which is phylogenetically related to

- hypoviruses but has a genome organization and gene expression strategy resembling those of plant potex-like viruses. *Mol. Cells*, 28, 73-74.
- Kwon, S.-J., Cho, S.-Y., Lee, K.-M., Yu, J., Son, M. and Kim, K.-H. (2009) Proteomic analysis of fungal host factors differentially expressed by *Fusarium graminearum* infected with *Fusarium graminearum* virus-DK21. *Virus Res.* 144, 96-106.
- Leal, J., Squina, F., Freitas, J., Silva E., Ono, C., Martinez-Rossi, N. and Rossi, A. (2009) A splice variant of the *Neurospora crassa hex-1* transcript, which encodes the major protein of the woronin body, is modulated by extracellular phosphate and pH changes. *FEBS letters*, 583, 180-184.
- Lee, K.-M., Yu, J., Son, M., Lee, Y.-W. and Kim, K.-H. (2011) Transmission of *Fusarium boothii* mycovirus via protoplast fusion causes hypovirulence in other phytopathogenic fungi. *PLoS ONE*, 6, e21629.
- Lin, Y., Son, H., Lee, J., Min, K., Choi, G. J., Kim, J.-C. and Lee, Y.-W. (2011). A putative transcription factor MYT1 is required for female fertility in the ascomycete *Gibberella zeae*. *PLoS One*, 6, e25586.
- Liu, F., Ng, S. K., Lu, Y., Low, W., Lai, J. and Jedd, G. (2008) Making two

- organelles from one: Woronin body biogenesis by peroxisomal protein sorting. *J. Cell Biol.* 180, 325-339.
- Managadze, D., Würtz, C., Sichting, M., Niehaus, G., Veenhuis, M. and Rottensteiner, H. (2007) The peroxin *PEX14* of *Neurospora crassa* is essential for the biogenesis of both glyoxysomes and woronin bodies. *Traffic*, 8, 687-701.
- Maruyama, J., Juvvadi, P. R., Ishi, K. and Kitamoto, K. (2005) Three-dimensional image analysis of plugging at the septal pore by woronin body during hypotonic shock inducing hyphal tip bursting in the filamentous fungus *Aspergillus oryzae*. *Biochem. Biophys. Res. Commun.* 331, 1081-1088.
- McCartney, A. W., Greenwood, J. S., Fabian, M. R., White, K. A. and Mullen R.T., (2005) Localization of the *Tomato bushy stunt virus* replication protein p33 reveals a peroxisome-to-endoplasmic reticulum sorting pathway. *Plant Cell*, 17, 3513-3531.
- Min, K., Lee, J., Kim, J.-C., Kim, S. G., Kim, Y. H., Vogel, S., Trail, F. and Lee Y-W. (2010) A novel gene, *ROA*, is required for normal morphogenesis and discharge of ascospores in *Gibberella zeae*. *Eukaryot. Cell*, 9, 1495-1503.
- Ng, S. K., Liu, F., Lai, J., Low, W. and Jedd, G. (2009) A tether for woronin

- body inheritance is associated with evolutionary variation in organelle positioning. *PLOS Genet.* 5, e1000521.
- Pathak, K. B., Sasvari, Z. and Nagy, P. D. (2008) The host Pex19p plays a role in peroxisomal localization of tombusvirus replication protein. *Virology* 379, 294-305.
- Pearson, M. N., Beever, R. E., Boine, B., and Arthur, K. (2009) Mycoviruses of filamentous fungi and their relevance to plant pathology. *Mol. Plant Pathol.* 10, 115-128.
- Rostagno, L., Crivelli, G. and Turina, M. (2009) Study of mRNA Expression by real time PCR of Cpkk1, Cpkk2 and Cpkk3, three MEKs of *Cryphonectria parasitica*, in virus-free and virus-infected isogenic isolates. *J. Phytopathol.* 158:409-416.
- Son, H., Lee, J., Park, A. R. and Lee, Y.-W. (2011a) ATP citrate lyase is required for normal sexual and asexual development in *Gibberella zeae*. *Fungal Genet. Biol.* 48, 408-417.
- Son, H., Seo, Y.-S., Min, K., Park, A. R., Lee, J., Jin, J.-M., Lin, Y., Cao, P., Hong, S.-Y., Kim, E.-K., Lee, S.-H., Cho, A., Lee, S., Kim, M.-G., Kim, Y., Kim, J. E., Kim, J.-C., Choi, G.J., Yun, S.-H., Lim, J. Y., Kim, M., Lee, Y.-H., Choi, Y.-D. and Lee, Y.-W. (2011b) A phenome-based functional analysis of transcription factors in the

- cereal head blight fungus, *Fusarium graminearum*. *PLoS Pathog.* 7, e1002310.
- Soundararajan, S., Jedd, G., Li, X., Ramos-Pamplona, M., Chua, N. H. and Naqvi, N. I., (2004) Woronin body function in *Magnaporthe grisea* is essential for efficient pathogenesis and for survival during nitrogen starvation stress. *Plant Cell*, 16, 1564-1574.
- Sun, Q., Choi, G. H. and Nuss, D. L. (2009) Hypovirus-responsive transcription factor gene *pro1* of the chestnut blight fungus *Cryphonectria parasitica* is required for female fertility, asexual spore development, and stable maintenance of hypovirus infection. *Eukaryot. Cell*, 8, 262-270.
- Suzuki, N., Maruyama, K., Moriyama, M. and Nuss, D. L. (2003) Hypovirus papain-like protease p29 functions *in trans* to enhance viral double-stranded RNA accumulation and vertical transmission. *J. Virol.* 77, 11697-11707.
- Tenney, K., Hunt, I., Sweigard, J., Pounder, J. I., McClain, C., Bowman, E. J. and Bowman, B. J. (2000) *Hex-1*, a gene unique to filamentous fungi, encodes the major protein of the woronin body and functions as a plug for septal pores. *Fungal Genet. Biol.* 31, 205-217.
- Tey, W. K., North, A. J., Reyes, J. L., Lu, Y. F. and Jedd, G. (2005)

- Polarized gene expression determines woronin body formation at the leading edge of the fungal colony. *Mol. Biol. Cell*, 16, 2651-2659.
- Wang, S., Kondo, H., Liu, L., Guo, L. and Qiu, D. (2013) A novel virus in the family *Hypoviridae* from the plant pathogenic fungus *Fusarium graminearum*. *Virus Res.* 174, 69-77.
- Wickner, R. B., Fujimura, T. and Esteban, R. (2013) Viruses and prions of *Saccharomyces cerevisiae*. *Adv. Virus Res.* 86, 1-36.
- Wolkow, T. D., Harris, S. D. and Hamer, J. E. (1996) Cytokinesis in *Aspergillus nidulans* is controlled by cell size, nuclear positioning and mitosis. *J. Cell Sci.* 109, 2179-2188.
- Wu, M., Zhang, L., Li, G., Jiang, D., Hou, M. and Huang, H.-C. (2007) Hypovirulence and double-stranded RNA in *Botrytis cinerea*. *Phytopathology*, 97, 1590-1599.
- Xie, J., Wei, D., Jiang, D., Fu, Y., Li, G., Ghabrial, S. A. and Peng, Y. (2006) Characterization of debilitation-associated mycovirus infecting the plant-pathogenic fungus *Sclerotinia sclerotiorum*. *J. Gen. Virol.* 87, 241-249.
- Xu, A., Jao, D. L. and Chen, K. Y. (2004) Identification of mRNA that binds to eukaryotic initiation factor 5A by affinity co-purification and differential display. *Biochem. J.* 384, 585-590.

- Yu, J., Kwon, S.-J., Lee, K.-M., Son, M. and Kim, K.-H. (2009) Complete nucleotide sequence of double-stranded RNA viruses from *Fusarium graminearum* strain DK3. *Arch. Virol.* 154, 1855-1858.
- Yu, J., Lee, K.-M., Son, M. and Kim, K.-H. (2011) Molecular characterization of *Fusarium graminearum* virus 2 Isolated from *Fusarium graminearum* strain 98-8-60. *Plant Pathology J.* 27, 285-290.
- Yu, X., Li, B., Fu, Y., Jiang, D., Ghabrial, S. A., Li, G., Peng, Y., Xie, J., Cheng, J. and Huang, J. (2010) A geminivirus-related DNA mycovirus that confers hypovirulence to a plant pathogenic fungus. *Proc. Nat. Acad. Sci. USA* 107, 8387-8392.
- Yuan, P., Jedd, G., Kumaran, D., Swaminathan, S., Shio, H., Hewitt, D., Chua, N. H. and Swaminathan, K. (2003) A HEX-1 crystal lattice required for woronin body function in *Neurospora crassa*. *Nat. Struct. Mol. Biol.* 10, 264-270.

CHAPTER II

**Hex1 protein binds specifically to both plus-strand
5' and 3' untranslated regions of the
Fusarium graminearum virus 1
and functions in viral RNA replication.**

ABSTRACT

The *HEX1* gene of *Fusarium graminearum* was previously reported to require for efficient *Fusarium graminearum* virus 1 (FgV1) RNA accumulation. To investigate whether Hex1 protein specifically binds to FgV1 viral RNA, we conducted electrophoretic mobility shift assays (EMSA) with recombinant Hex1 protein and RNA transcripts corresponding to the various regions of FgV1 genomic RNA. These analyses demonstrated that Hex1 protein specifically binds both 5'- and 3'- untranslated regions (UTR) of plus-strand genomic RNAs. To further verify whether Hex1 affect FgV1 replication, we carried out quantification of both (+) and (-) strand viral RNA in protoplasts using virus-infected wild-type, *HEX1* gene deletion, and Hex1 over-expression strains. Northern blot analysis and first-strand qRT-PCR results showed that both plus- and minus-strand of FgV1 RNA was substantially increased in over-expression strain. These studies indicated that the Hex1 function in FgV1 replication by binding to the 5'- and 3'-UTR of FgV1 genomic RNA.

INTRODUCTION

All viruses are relatively gene poor comparing with their hosts. For maintaining the infection cycles of viruses in host cells, viruses must utilize various elements from host which play essential role(s) in virus infection. Thus, the most important task for virus is interaction between viral elements and host factors through the all viral infection steps. Consequently, ascertain of such host factors and their contributions have been appreciated as a long-time issue.

Although host factor researches for mycovirus (fungal virus) are not sufficient as compared with those of plant and animal virus, several host factors required for viral life in host cell were identified and characterized in *Cryphonectria hypovirus 1*-EP713 (CHV1) of the chestnut blight fungus, *Cryphonectria parasitica*. As a model system for study about mycovirus-host interaction, CHV1 - *C. parasitica* system has been contributed for a long time. One of the first identified host factor is NAM-1 which is associated symptom expression to CHV1 (Faruk et al., 2008). The *C. parasitica* gene *pro1* was identified and characterized as a host factor required for the maintenance of CHV1 infection (Sun et al., 2009). Other host gene *Cpbir1* associated with hypovirus infection and hypovirus

transmission is recently reported (Gao et al., 2012).

Fusarium graminearum virus 1 strain DK21 (FgV1) is a RNA virus that infects a devastating plant-pathogenic fungus *F. graminearum*, the causal agent of cereal head blight on small grains such as barley and wheat (Son et al., 2011). When FgV1 infects the host fungus, virus infection leads to reduction the virulence (hypovirulence) of *F. graminearum* and also delayed mycelial growth, increased pigmentation, and reduced production of mycotoxin (Chu et al., 2002). The FgV1 consists of about 6.6-kb, excluding the 3'-terminal poly (A) tail. The viral RNA has 53- and 46-nucleotide 5'-and 3'-untranslated region (UTR) , respectively, that might play important roles for viral protein translation and viral RNA replication as reported for many other in RNA viruses (Kwon et al., 2007, Shi et al., 2006). Among these viruses, so many roles of UTRs have been demonstrated with Hepatitis C virus (HCV). These RNA elements play roles as initiation sites for viral protein translation and RNA replication by interaction each other or binding viral and/or cellular proteins (Shi et al., 2006).

It has recently been reported the cellular functions of a *Fusarium graminearum* gene, *HEX1*, which is required for asexual reproduction, cellular integrity, and pathogenesis. Hex1 is also required for efficient viral RNA accumulation as a host factor of FgV1 (Son et al., 2013). The *HEX1*

gene encodes about 20 kDa protein which is major constituent of woronin body, small dense core organelle found at near septa in typical filamentous fungi such as *Neurospora crassa*, *Magnaporthe oryzae* and *F. graminearum* (Jedd et al., 2000, Son et al., 2013, Soundararajan et al., 2004). And the protein tertiary structure study revealed crystal structure of Hex1 protein has structural homology with eukaryotic initiation factor 5A (eIF-5A) (Yuan et al., 2003). It is widely known that the eIF-5A protein is involved in first peptide bond formation and cell-cycle regulation (Henderson et al., 2011). Additionally, homology based structure prediction study demonstrated that eIF-5A has two RNA-binding folds which are preserved well in Hex1 protein (Peat et al., 1998). These RNA-binding folds clearly suggested that Hex1 protein may bind to FgV1 RNA and play a role(s) for viral RNA replication.

In this chapter, I report experimental evidences that showing the Hex1 protein specifically bind to plus-strand of FgV1 RNA by conducting electrophoretic mobility shift assay (EMSA). I also demonstrate that Hex1 protein enhances the viral RNA replication of FgV1 in *F. graminearum*. This is the first report about regulation of RNA replication by fungal cellular protein which can directly interact with mycovirus RNA.

MATERIALS AND METHODS

I. Fungal strains and culture conditions

All strains used in this study (Table 1) were stored in 25% (v/v) glycerol at -80°C and were reactivated on potato dextrose agar (PDA; Difco). For nucleic acid manipulation, all strains of *F. graminearum* were grown in 50 ml of a liquid complete medium [CM, (Son et al., 2013)] at 25°C with shaking (150 rpm) for 5 days. Mycelia were harvested by filtration through miracloth (Calbiochem) and ground to a fine powder with liquid nitrogen in a mortar and pestle.

II. Computational analysis

Nucleotide sequences from the NCBI database were assembled using the Seqman program in DNASTAR (<http://www.dnastar.com>). Sequence similarity searches of *HEX1* and translational initiation factors 5A were conducted with the NCBI BLAST program. The alignment of Hex1 and translational initiation factors 5A amino acid sequences was performed by the MegAlign program in DNASTAR, using a default setting and GeneDoc programs (<http://www.nrbsc.org/gfx/genedoc>).

Protein structure prediction was performed using the SWISS-MODEL

workspace (<http://swissmodel.expasy.org>) according to previous report (Henderson et al., 2011). Predicted tertiary structures of FgHeX1 and FgIF5A were generated based on homology modelling comparing with Hex1 of *N. crassa* (PDB entry 1KHI) and *M. jannaschii* (PDB entry 1BKB), respectively (Yuan et al., 2003). Figures depicting molecular structure were prepared using PyMOL program (The PyMOL Molecular Graphics System).

III. Preparation of protoplast and total RNA extraction

Protoplasts of the all virus infected strains were prepared by treating fresh mycelia grown in CM liquid culture for 4 h at 30°C with 1 M NH_4Cl containing 50 mg/ml of driselase (InterSpex Products) as previously described with modification (Son et al., 2013). Protoplast were harvested by centrifugation at $2,544\times g$ at 4°C for 10 min, washed twice with STC (1.2M Sorbitol, 10mM Tris-HCl pH 7.5, 50mM CaCl_2), and suspended in 500 μl of MMC buffer (0.6M Mannitol, 10mM MOPS pH 7.0, and 10mM CaCl_2). Each protoplast suspensions were incubated at 25°C following different time point (0, 18, 36 h) and harvested by centrifugation at $800\times g$ at 4°C for 5 min.

For total RNA preparation, the powdered mycelia or harvested protoplasts were suspended in Isol-RNA lysis reagent (5 PRIME). Nucleic

acid was extracted by following the manufacturer's protocol with slight modification. The extracted total RNAs were purified twice with acid phenol:chloroform (1:1), precipitated with isopropanol, suspended in DEPC-treated water, and further treated with TURBO DNA-free™(Ambion) to remove genomic DNA.

IV. Plasmid construction and RNA transcription

Plasmid constructs were generated by digestion of the parent plasmid, pUC19 with *EcoR* I and *BamH* I. The positive and negative strand from each regions of FgV1 were amplified by PCR and ligated with digested pUC19 plasmid. All constructs were inserted to downstream of bacteriophage T7 promoter (Fig. 3A). These plasmids were then linearized with *BamH* I before being used as templates for *in vitro* synthesis of positive and negative strand RNAs.

The [³²P]-labeled RNA probes were obtained by transcription in the presence of 25 µCi [³²P] dCTP (3000 Ci/mmol; Perkin Elmer), 20 µM CTP, and 400 µM each ATP, GTP, UTP using linearized clones. Transcribed RNAs were purified twice with acid phenol:chloroform (1:1), precipitated with ethanol and 3 M NaOAc, suspend in 1 × EMSA binding buffer [10 mM Tris-HCl (pH 7.5), 10 mM MgCl₂, 100 mM KCl, 10mM DTT, 10%

glycerol].

V. Hex1 protein expression in *E. coli*

The full-length *F. graminearum* *HEX1* gene was cloned into pET-28a(+) vector (Novagen) between *EcoR* I and *Bam*H I restriction enzyme sites, and the resulting plasmid was transformed in to *E.coli* strain BL21-CodonPlus[®]-RIL competent cell. Cells were grown at 37 °C in LB medium to an optical density of 0.6 at 600 nm and induced with 0.4 mM IPTG. The collected cells were lysed by sonication in buffer containing 20 mM NaH₂PO₄·H₂O, 500 mM NaCl and 20 mM Imidazole (His-tag column binding buffer). After removing cell debris by centrifugation, the Hex1 protein in supernatant was purified using His GraviTrap (GE Healthcare). The eluted Hex1 protein was desalted using PD-10 desalting column (GE Healthcare). The final protein was eluted in 1 × EMSA binding buffer.

VI. Electrophoretic mobility shift assays

The EMSA experiments were carried out as described by earlier report (Kim et al., 2002) with slightly modifications. The 10 ng of uniformly labeled RNA transcripts were incubated with Hex1 protein on ice in a final volume of 10 µl of 1 × EMSA binding buffer. The reaction mixtures were mixed

with 0.2 volume of $5 \times$ loading buffer (50% glycerol and 0.05% bromophenol blue) and analyzed on a 5% non-denaturing polyacrylamide gels made in $0.5 \times$ TBE. The samples were electrophoresed at 100 V (4°C) for 40min. The gels were dried completely using vacuum dryer. The images were visualized using a Fuji BAS-2500 Phosphor Imager and corresponding imaging software (Fuji). The relative intensities of bands corresponding to RNA-protein complexes were determined by TotalLabQuant software (TotalLabQuant).

VII. Fungal protein extraction and western blot analysis

For fungal protein extraction, the powdered mycelia were suspended with lysis buffer (Son et al., 2013). This lysate was filtered twice through miracloth, and the filtrate was centrifuged at $100\times g$ for 5 min to remove unlysed cells. The lysate was then centrifuged at $10,000\times g$ for 5 min, and the pellet was suspended in lysis buffer. A 200- μ g quantity of total protein was resolved on a Mini-PROTEAN® TGX™ Precast gel (Bio-Rad) and transferred to a Hybond-P membrane (GE Healthcare) in transfer buffer (25mM Tris, 380mM glycine, 20% methanol) at 100 V for 40min for protein blot analysis. The membrane was blocked for 16 h in tris-buffered saline-Tween 20 (TBST) plus 2.5% skim milk (10 mM Tris pH 7.4, 100

mM NaCl, 0.05% (v/v) Tween-20). The membrane was then probed with anti-Hex1 antibody (1:200) in TBST plus 1% skim milk for 1 h at room temperature. The membrane was washed five times with TBST over the course of 1 h and probed with horseradish peroxidase-conjugated anti-rabbit IgG secondary antibody at 1:2000 dilution for 1 h. The membrane was then washed five times in TBST over the course of 1 h and evaluated for chemiluminescence using the Amersham ECL Western blotting detection reagents and analysis system (GE Healthcare) according to the manufacturer's protocol.

VIII. qRT-PCR and Northern blot analysis

The first-strand cDNAs were synthesized with SuperScript® III First-Strand Synthesis System for RT-PCR (Invitrogen) and viral RNA specific primers to quantify strand specific viral RNA accumulation. Quantitative real-time RT-PCR (qRT-PCR) was performed on a CFX96 Real-Time PCR System (Bio-Rad) using the SsoFast™ EvaGreen® Supermix (Bio-Rad) according to manufacturer's instructions. After initial denaturation at 95°C for 10 min, 40 cycles consisted of 5 s at 95°C and 5 s at 58°C. Two endogenous reference genes, cyclophilin 1 (*CYP1*, locus FGSG_07439) and elongation factor 1 α (*EF1 α* , locus FGSG_08811), were used in each experiment. The

PCR primers used in this study (see Table X in the supplemental material) were produced at an oligonucleotide synthesis facility (Bioneer).

For the Northern blot analysis, the 5 µg of extracted total RNAs were analyzed on 1 % denaturing agarose gel containing MOPS and formaldehyde. The RNA samples were electrophoresed at 60 V for 4 h and further gels were soaked twice denaturing solution (3 M NaCl and 0.01 N NaOH) for 15 min and 20 min at room temperature. The gels were capillary blotted onto positively charged nylon membranes (GE Healthcare) in 3 M NaCl and 0.01 N NaOH for 12 h. The [³²P]-labeled RNA probes were generated *in vitro* transcription and described above. The hybridization reaction was performed at 42°C for 16 h. After hybridization, unhybridized RNA probe was removed by washing with low (2x SSC and 0.1% SDS) and high (0.1x SSC and 0.1% SDS) stringency buffers. The blotting image was visualized using a Fuji BAS-2500 Phosphor Imager and corresponding imaging software (Fuji).

Table 1. Fungal strains used in this study.

Strain	Description	Reference
WT-VF	Wild type (WT), virus-free; Lineage 3	Son et al., 2013
WT-VI	WT-VF, infected with FgV1	Son et al., 2013
$\Delta hex1$ -VF	<i>HEX1</i> deletion mutant	Son et al., 2013
$\Delta hex1$ -VI	<i>HEX1</i> deletion mutant infected with FgV1	Son et al., 2013
<i>HEX1 OE-VI</i>	<i>HEX1</i> overexpression mutant infected with FgV1	Son et al., 2013
$\Delta hex1::HEX1$ -VI	<i>HEX1</i> complemented mutant infected with FgV1	Son et al., 2013

RESULTS

I. Structure of Hex1 protein and homology with eIF-5A

Computer based comparison of the deduced amino acid sequence of *F. graminearum* Hex1 revealed high level of sequence identity with *N. crassa* Hex1 (72%), but not that much high with IF-5A from *F. graminearum* (21%), *Pyrobaculum aerophilum* (10%), and *Methanococcus jannaschii* (12%). Despite the low levels of sequence identities among FgHex1 and IF-5As, all proteins were structurally overlapped with high score using the SSAP server of CATH (Fig. 1; Arnold et al., 2006).

The homology based protein structure prediction demonstrated both FgHex1 and FgIF-5A have two-domain structures consisting of mutually perpendicular antiparallel β -barrels (Fig. 2, panels A and B). Six antiparallel β -strands and one helix made the N-terminal barrel. The C-terminal domain consisted of five β -strands and two helices. Comparison of the Hex1 structure and that of IF-5A revealed that these two different proteins share a similar structural organization (Fig. 2C).

II. Purification of Hex1 protein from *E. coli* and western blot analysis

Expression and purification of the recombinant Hex1 protein from *E. coli*

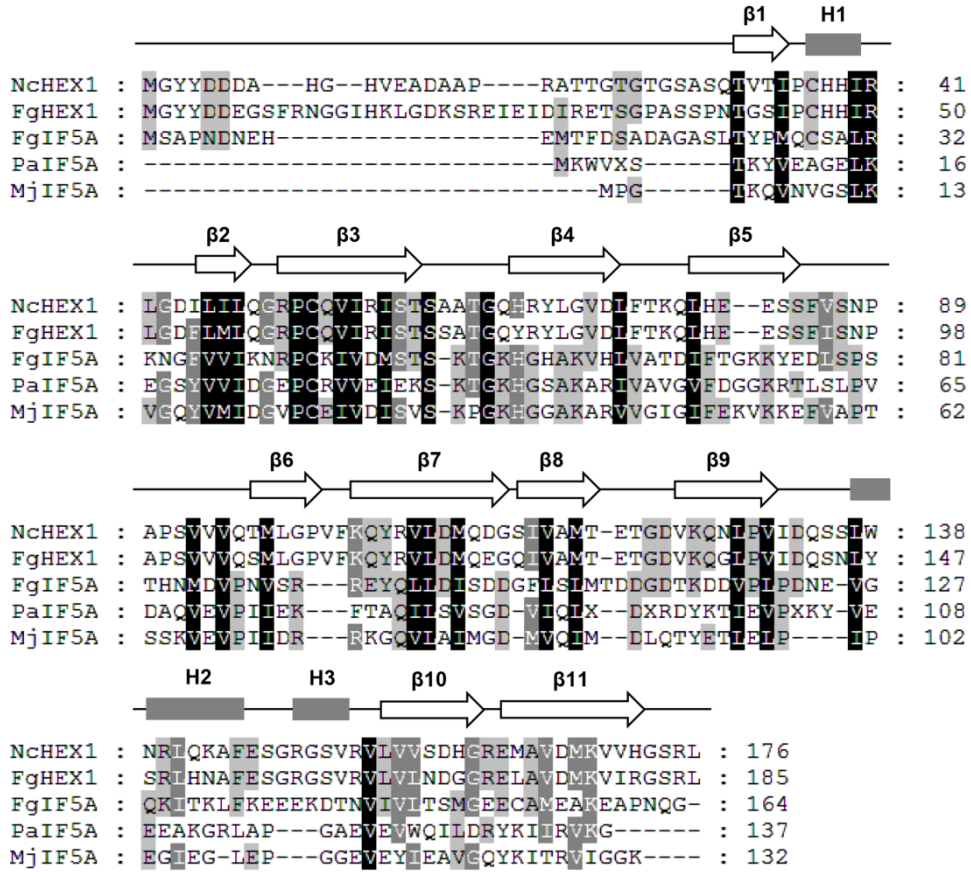


Fig. 1. Deduced amino acid sequence alignment of Hex1 from *N. crassa* (NcHex1), *F. graminearum* (FgHex1) and IF-5A from *F. graminearum* (FgIF5A), *P. aerophilum* (PaIF5A), *M. jannaschii* (MjIF5A). The alignment was conducted using MegAlign in Lasergene, using default setting. Secondary structure elements designated by empty arrows for β -strands and grey box for helices. For the letters above the arrows and boxes, H refers to the helix-turn-helix and β refers to the beta sheet.

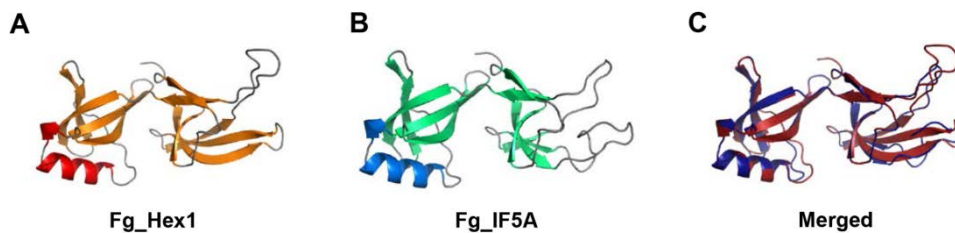


Fig. 2. Predicted structures of Hex1 and IF-5A. (A) Overall structure of FgHex1. The helices are shown in red; and the β -strands, in orange. (B) Overall structure of FgIF5A. The helices are shown in sky blue; and the β -strands, in green. (C) Merged structure of FgHex1 and FgIF5A. The FgHex1 is shown in red; and the FgIF5A, in dark blue. All proteins are composed of two mutually perpendicular antiparallel β -barrels.

were carried out as describe above (see Materials and Methods). Cellular FgHex1 protein was a polypeptide with 186 amino acids and a molecular mass of about 20 kDa (Fig. 3A, lane WT-VF). However, additional nucleotide sequences in cloning into expression region of pET-28 a(+) vector was added and thus increased the molecular mass of recombinant Hex1 protein by about 5 kDa.

Western blot analysis was carried out to verify whether expressed protein was Hex1 or not using anti-HEX1 antibody. One major band with molecular mass of approximately 20 kDa from cellular fungal protein loaded lane and 25 kDa from *E. coli* total protein loaded lanes were detected except the deletion mutant strain (Fig. 3B). Only one protein band was detected from his-tag column purified protein (Fig. 3B, lanes Hex1-HE1 and Hex1-HE2).

III. Plasmid construction and Hex1 protein manipulation

To further prepare for confirming the physical interaction between FgHex1 and FgV1 viral RNA, eleven plasmids which can utilize preparation of RNA probe as a template were constructed. A set of eleven plasmids could transcribe both plus- and minus- strands of various FgV1 viral RNA regions

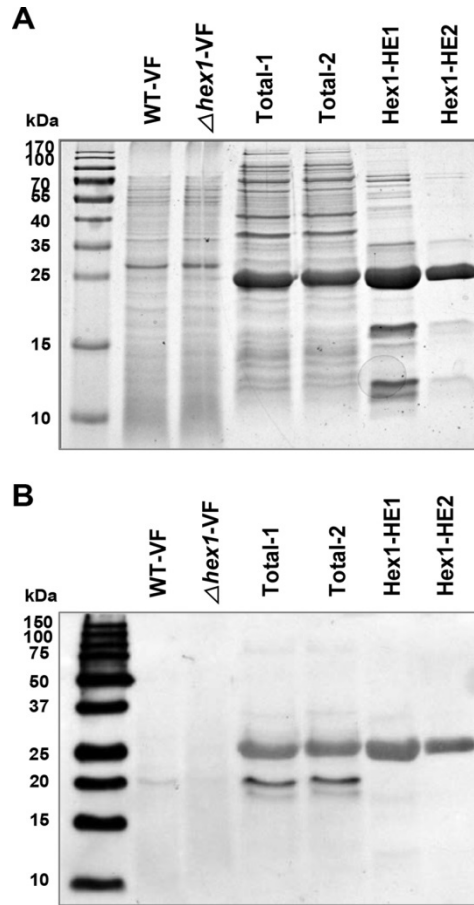


Fig. 3. *E. coli* expression of Hex1 and western blot analysis. (A) Recombinant Hex1 protein expression in *E. coli*. Fungal total protein extracted from WT-VF and $\Delta hex1$ -VF strain for experimental control. Extracted *E. coli* total protein designated for Total-1, -2. Purified using HisGraviTrap Hex1 protein designated by Hex1-HE1, -HE2 and E1, E2 refer the elution order. All samples were then separated by 12% SDS-PAGE gel and stained by Coomassie blue staining (B) or blotted onto Hybond-P membrane. The blot was probed with anti-Hex1 antibody. The positions of the molecular mass markers are shown on the left of panel A and B.

under control of bacteriophage T7 promoter in RNA transcription (Fig. 4A). Hex1 protein was also manipulated to desalting, buffer exchange and protein clean up using PD-10 Desalting columns. After elution, Hex1 protein band was detected on SDS-PAGE gel (Fig. 4B).

IV. Specific binding of Hex1 to both 5' and 3' UTR of FgV1 plus-strand RNA

To determine whether Hex1 protein bind to FgV1 viral RNA, EMSA was carried out with RNA probes derived from different region of FgV1 genome. The result showed that 5'-and 3'-UTR of plus-strand RNA formed a complex with slower electrophoretic mobility comparing with that of central region derived plus-strand RNA (Fig. 5, top panels). While the levels of Hex1 protein increased by gradually (from 25 nM to 300 nM), the remained free RNA probes were decreased consequently only in condition which both UTRs of plus-strand RNA used as a probe (Fig. 6). By contrast, delayed migrations and decreased the level of free RNA probes were not detected when minus strand RNAs were used as a probe (Fig. 5, low panel).

Additionally, EMSA was performed with both plus and minus RNA probe derived from 5' region of subgenomic RNA 1 and 2. Those RNAs

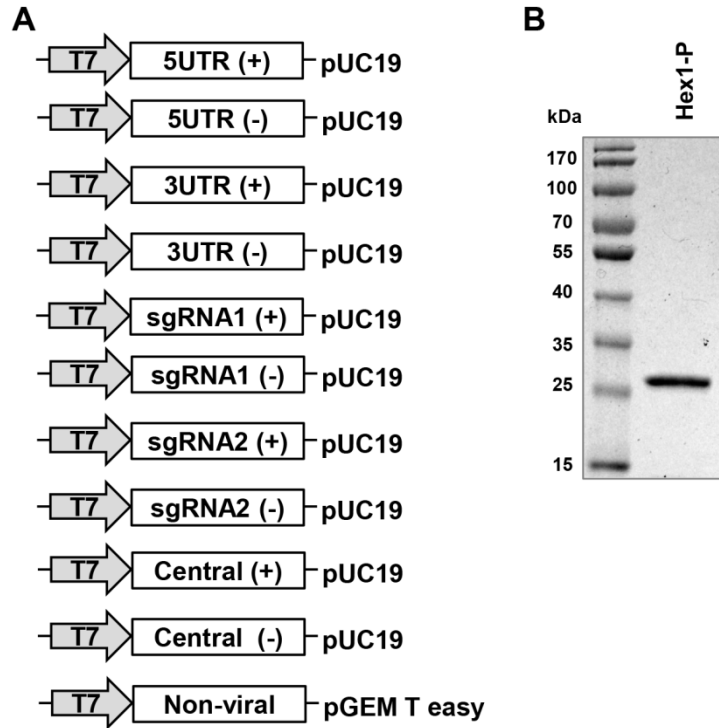


Fig. 4. Construction of plasmid and Hex1 protein manipulation (A) Schematic representation of constructs used *in vitro* transcription for EMSA. All plasmid constructs contains bacteriophage derived T7 promoter for transcription and further linearized by restriction enzyme. For the letters in the boxes right after T7 promoter (grey arrow) refer various region of FgV1. All plasmids were generated based on pUC19 excluding Non-viral construct. (B) PD-10 desalting column purified Hex1 protein. Purified protein was analyzed on a 12% SDS-PAGE gel and further stained by Coomassie blue staining. The positions of the molecular mass markers are shown on the left of panel B.

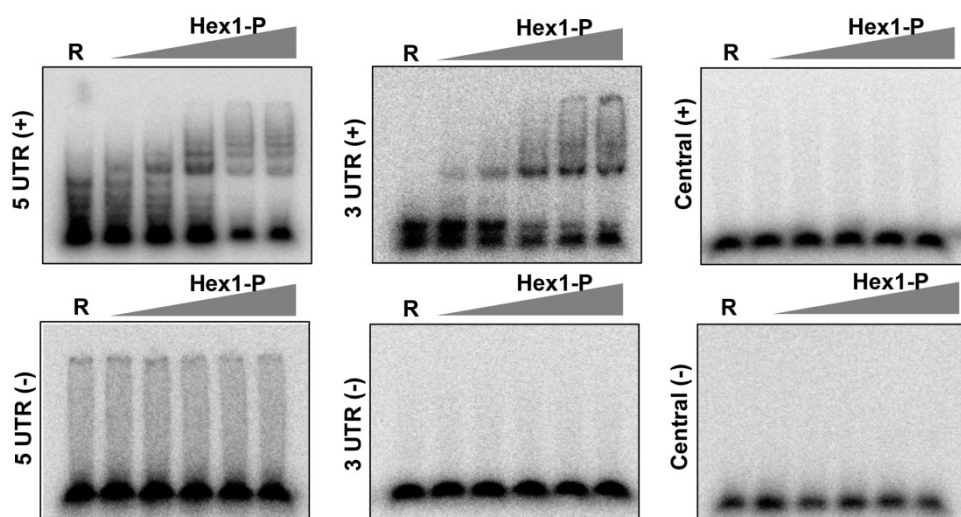


Fig. 5. Investigation of direct interaction using RNA-protein complexes formation. (A) Electrophoretic mobility shift assay (EMSA) of FgV1 RNA-Hex1 protein complexes. For the letter and figure above the image, R refer RNA probe only in lane and a grey right-angled triangle refers increment of Hex1 concentration. The letters on the left side of images refer RNA probes derived from various region of FgV1 genome.

not form complex showing delayed migration on gel (Fig. 7).

V. Strand specific quantification of FgV1 viral RNA accumulation

Northern blot analysis was performed to investigate whether Hex1 protein influences FgV1 viral RNA by strand specific manner. Northern blot and results showed both plus-strand of viral RNA accumulated high in *HEX1 OE-VI* strain and low in $\Delta hex1$ -VI strain comparing with WT-VI strain at 5 d.p.i. (Fig. 8, left panel). The accumulation of minus strand viral RNA also showed similar pattern, greater in overexpression strain and lower in deletion strain, with that of plus-strand viral RNA (Fig. 8, right panel).

Quantitative RT-PCR was carried out to quantify the level of both plus and minus viral RNA accumulation. The qRT-PCR analysis revealed that plus viral RNA accumulated more than 2.5-fold greater in the *HEX1 OE-VI* strain and 3-folds lower in the $\Delta hex1$ -VI than in the WT-VI strain at 5 dpi. (Fig. 9). Relative to the minus viral RNA accumulation in the WT-VI, the level was decreased by approximately 3-folds in the $\Delta hex1$ -VI and increased by 2.5-fold in *HEX1 OE-VI* (Fig. 9). In all strain, plus-strand viral RNA accumulated more than at least 2.5-fold than minus-strand viral RNA (Fig. 9).

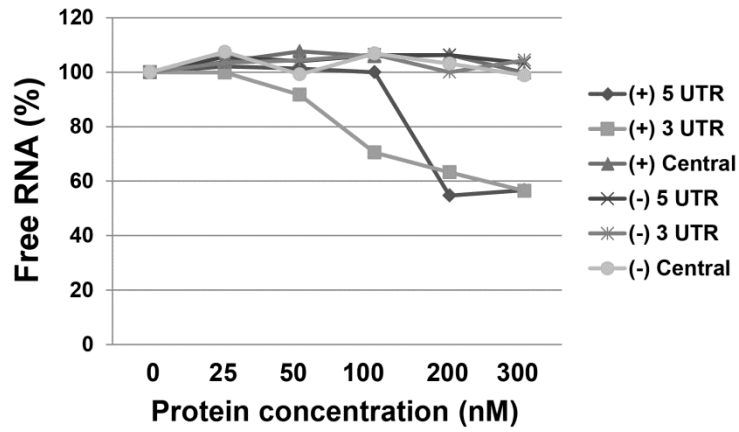


Fig. 6. Relative free RNA probes in EMSA experiments. The band intensities of free RNAs were determined using image quantification software, TotalLabQuant. Each lanes of R set at 100% for each experiment.

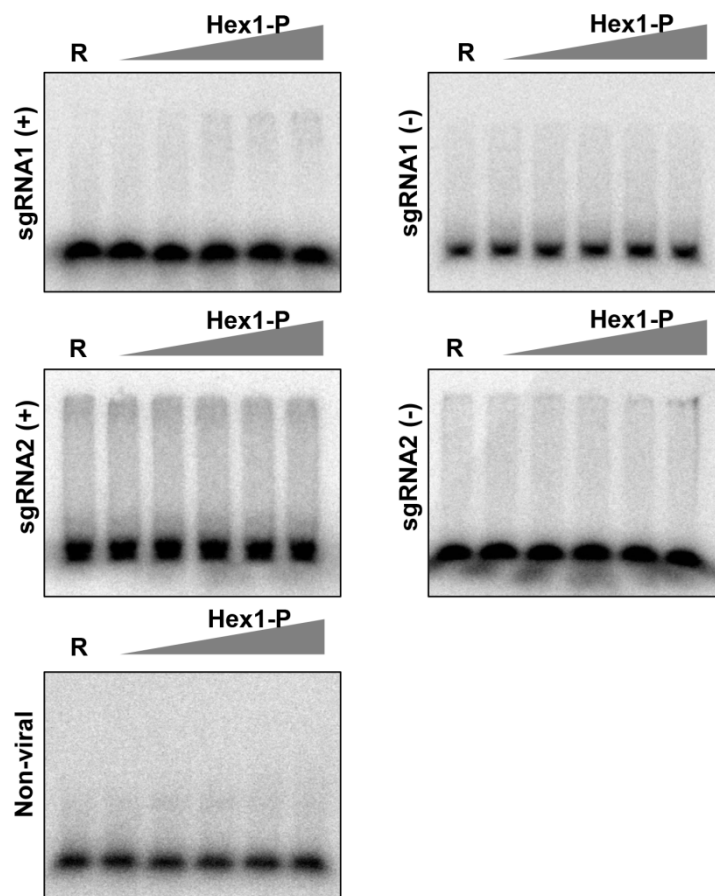


Fig. 7. Electrophoretic mobility shift assay (EMSA) of FgV1 RNA-Hex1 protein complexes. For the letter and figure above the image, R refer RNA probe only in lane and a grey right-angled triangle refers increment of Hex1 concentration. The letters on the left side of images refer RNA probes derived from various region of FgV1 genome.

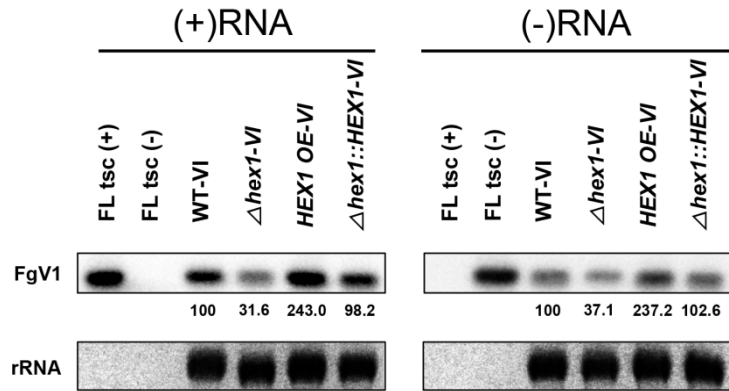


Fig. 8. Plus- and minus-strand RNA accumulation in all virus-infected strains. (A) Investigation of viral RNA accumulation in the WT-VI, Δ hex1-VI, *HEX1 OE-VI*, and Δ hex1::*HEX1-VI* at 5 dpi. using northern blot analysis. Different ssRNA probes were used for detection plus- and minus-strand viral RNA accumulation. The values above the blot images represent the percentage of ssRNA compared to the accumulation of WT-VI, which is set at 100% for ssRNA. The band intensities of free RNAs were determined using image quantification software, TotalLabQuant.

VI. The effect of Hex1 on strand specific RNA synthesis in protoplast

For the investigation of plus-and minus-strand RNA synthesis levels excluding viral RNA accumulation related molecular mechanism in host cell such as cell to cell movement and others, total RNAs were extracted from protoplasts of virus infected *F. graminearum* (see Materials and Methods). The levels of both strands viral RNA synthesis were determined by northern blot analysis and qRT-PCR at different time point. The northern blot and qRT-PCR results showed that after incubating for 36 h, both plus- and minus-strands of viral RNAs from all virus infected strains were slightly increased to a greater or lesser degree (Fig 10 and 11). The plus viral RNA of *HEX1 OE-VI* increased greater than those of others at 18 h to 36 h. In at 18 h and 36 h was dramatically increased by approximately 1.7-fold (Fig. 11, left panel). In contrast, in the $\Delta hex1$ -VI, both plus- and minus-strands viral RNA detected at the least amount and the increment levels were substantially low at 18 h to 36 h among the other strains (Fig 10 and 11). particular, the increment level of plus-strand viral RNA in the *HEX1 OE-VI*

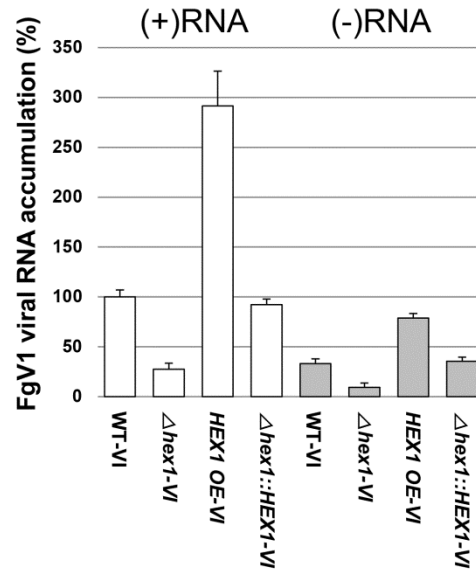


Fig. 9. Relative plus-and minus-strand viral RNA accumulation in all virus-infected strains of *F.graminearum*. Relative transcript levels were normalized using cDNA of elongation factor 1 α and cyclophilin 1. Error bars indicate standard deviation. All values are significantly different at $p<0.05$ based on the Tukey test.

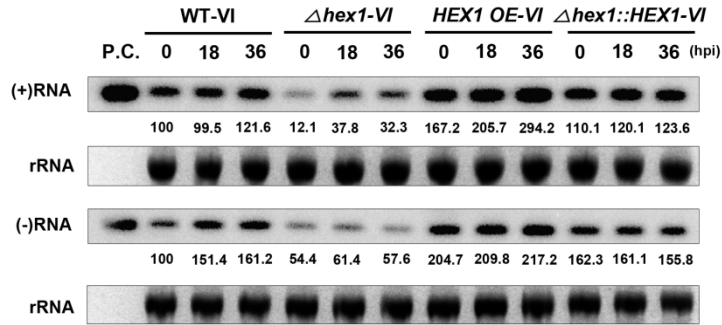


Fig. 10. Time course mediated quantification of FgV1 viral RNA replication in virus-infected *F. graminearum* protoplasts. (A) Northern blot analysis of FgV1 viral RNA accumulation in protoplast from WT-VI, $\Delta hex1$ -VI, OE-VI, and $\Delta hex1::HEX1$ -VI strains. The values above the blot images, 0, 18 and 36 refer incubation time of protoplasts. The values below the blot images represent the percentage of ssRNA compared to the accumulation of WT-VI in 0 h, which is set at 100% for ssRNA. The band intensities of free RNAs were determined using image quantification software, TotalLabQuant.

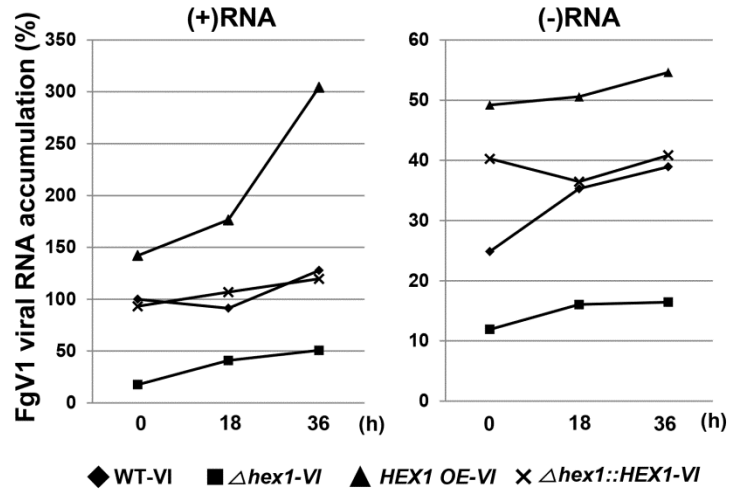


Fig. 11. Relative plus-and minus-strand viral RNA accumulation in all virus-infected protoplasts. Graphs are separated by two for convenience. Error bars indicate standard deviation. All values are significantly different at $p < 0.05$ based on the Tukey test.

DISCUSSION

Present study indicates that a 20-kDa host factor, Hex1 protein, can directly interact with at least two sites (both 5'-and 3'-UTR of plus-strand RNA) of FgV1 viral RNA. For investigating the obtained result, I introduced *in vitro* accesses such as protein structure prediction, fungal protein expression in bacterial cell and RNA-protein binding assay. Moreover, I also confirmed that this protein-RNA interaction facilitates plus-strand RNA synthesis in FgV1 infected *F. garminearum*. In previous study from our laboratory, I demonstrated that FgV1 viral RNA accumulated by *HEX1* gene dependent manner in 5 days incubation of liquid culture and plate culture condition. The accumulation level of FgV1 RNA increased in *HEX1* over-expression strain and decreased in deletion strain as compared with WT-VI strain. Taken together both studies, these distinct accumulations came from relatively much more plus RNA synthesis facilitated by Hex1 protein.

According to the pre-existing researches results about HEX1 from various filamentous fungi, *HEX1* genes encode about 20-kDa protein known as major constituent of woronin body (WB), dense-core vesicle specific to filamentous fungi (Jedd et al., 2000, Son et al., 2013, Soundararajan et al.,

2004). The WB functions to seal the septal pore responding to cellular damage (Jedd et al., 2000). However, leaving without a concerning about cellular function of Hex1 protein, one remarkable finding is that Hex1 shares homology with eIF-5A structurally and sequentially (Fig. 1 and Yuan et al., 2003). The eIF-5A is a highly conserved protein in all organisms ranging from archaeobacterial and mammals. This small (~17 kDa) acidic protein contains the unusual amino acid residue, hypusine (Saini et al., 2009). The eIF-5A plays roles in the formation of the first peptide bond during translation, in cell cycle progression of yeast and mRNA decay (Henderson et al., 2011, Li et al., 2010, Saini et al., 2009, Preiss et al., 2003, Zanelli et al., 2007). The most important thing that captured our attention is that eIF-5A have RNA binding folds which consisted of aromatic rings (Trp, Tyr) and positively charged residue (Lys, Arg) (Peat et al., 1998). These literature studies strongly suggested that Hex1 protein might bind to FgV1 viral RNA and involved in viral RNA accumulation

The EMSA results clearly showed that Hex1 protein specifically bind to plus-strand of both UTRs (Fig. 5). The more RNA-protein complexes were formed while increasing Hex1 concentration from 25 nM to 300 nM (Fig. 5 and 6). Even though the assay was carried out in high concentration of Hex1 (over 300 nM), RNA-protein complex formation was not detected excepting

plus-strand of both UTRs RNA probes conditions in repeated experiments (data not shown). Our previous qRT-PCR result demonstrated that FgV1 RNA accumulation level is substantially high in *HEX1* over-expression fungal strain and low in deletion strain comparing with WT-VI strain after 5 days incubation (Son et al., 2013). Taken together, these combined data indicated that RNA-protein complexes formation increases with Hex1 concentration increased and such trend of direct interaction between Hex1 and FgV1 involved in FgV1 viral RNA accumulation.

In accordance with a previous study about *HEX1* gene (Son et al., 2013), an incubation period of 5 days is accorded for all virus-infected fungal strains. The northern blot analysis and first strand qRT-PCR result informed each strands of viral RNAs were accumulated in a similar trend with previous qRT-PCR result (Fig. 9 and Son et al., 2013). Additionally, first strand qRT-PCR result enables that estimation of accumulated plus-and minus-strand viral RNA is approximately 3 in all virus infected strains (Fig. 9). Although this is the first report about separated quantification of both plus and minus RNAs affected by host protein in dsRNA mycovirus infected filamentous fungi, however, I could not determine what kind(s) of RNA metabolism does/do affect these accumulation patterns of FgV1 RNAs. Therefore, I decided to introduce a protoplast system for studying

replication of FgV1. However, RNA transfection or DNA clone insertion mediated mycovirus infection to fungal transformation is currently unavailable. So, protoplasts were generated from fresh grown mycelia with slightly modified typical protocol used for single conidia (see Materials and Methods). By using the method developed, initial infection step is not required. Because protoplasts were derived from virus-infected mycelia. However, efficiency of protoplast from mycelia is low in comparison with that from conidia and more time and driselase consuming. Although there are some disadvantages, levels of both plus and minus RNA synthesis after different incubation time (0, 18, 36 h) were successfully determined using northern blot and first-strand qRT-PCR. In addition, the reasons why I set these three time points are derived from previous studies. Previously, molecular characterization of FgV1 suggested that genome structure of FgV1 is similar with that of plant potex-like virus (Kwon et al. 2007). In case of *Potato virus X* (PVX), one of the well-known viruses in genus *potexvirus*, accumulation level of genomic plus-strand RNA in plant protoplasts increased rapidly at 24 to 48 hpi (Park et al., 2009) and accurate quantification of plus-strand RNAs enables after 6 h because of hindrance by presence of input RNA (Kim et al., 1996). Therefore, I set our time points 0 h to quantify pre-existing viral RNA, 18 h and 36 h for expecting

rapidly increased time point in our system, respectively.

In nature of dsRNA in host cell, virus replicates through plus-strand RNA to complete viral life. These replicated plus RNAs play like cellular mRNA and further utilize for translation as a template. In parallel, these RNAs packaged by the resulting viral protein from translation and then produce new virions for progeny virus (Ahlquist et al., 2006, Jackson et al., 2011, Mellits et al., 1998). Therefore, it is generally accepted that plus-strand RNA synthesis is the decider of viral life cycle in host cell. Our northern blot and first-strand qRT-PCR result using protoplast RNAs demonstrated that plus RNA in *HEX1 OE-VI* strain increased rapidly after 18 h incubation. These combined data suggested that host protein Hex1 involves in dsRNA virus replication cycle, especially in plus RNA synthesis step.

Although present study demonstrated that cellular protein affects plus-strand RNA synthesis in viral replication cycle by direct interaction, it still has a chance to additional function(s) related to viral life in host cell. I speculate that Hex1 protein functions in translation of viral protein. Hex1 binds to both 5'-and 3'-UTR of plus-strand RNA, as revealed in this study.

In particular, 5'-UTR is the initiation site of both viral replication and translation (Ahlquist et al., 2003, Shi et al., 2006, Jackson et al., 2010,

Mellits et al., 1998). Therefore, host protein bind to 5'-UTR of viral RNA and then affect viral translation. RNA-binding protein G-rich sequence factor 1 (GRSF-1) binds to 5'-UTR of influenza virus and stimulate viral protein translation (Park et al., 1999). And 3'-UTR is also binding site for cellular protein which affecting viral translation. Poly(A)-binding protein (PABP) binds to non-polyadenylated 3'-UTR of dengue virus (DENV) and then enhances viral translation (Polack et al., 2009). Here, several cellular proteins such as ATP-dependent RNA helicase DDX6 (RpK/p54 protein), U6 snRNA-associated Sm-like protein (LSm1) and DNA topoisomerase 2-associated protein (PAT1) which can bind both UTRs and affect viral replication and translation of HCV (Scheller et al., 2009, Galão et al., 2010). Here, identified roles of these cellular proteins from other organisms and identical binding sites for Hex1 provide the suspecting that Hex1 functions as a host factor affecting viral protein translation.

A second speculation of Hex1 function is role(s) for protection of viral RNA from cellular RNA decay machinery. In general, exoribonuclease and exosome play each role in the 5'-to-3' and 3'-to-5' mRNA decay pathway, respectively (Dickson et al., 2011, Moon et al., 2012). RNA viruses always

try to avoid these mechanisms for survival in host cell. Binding of Human antigen R (HuR) protein to 3'-UTR of Sindbis Virus (SinV), for example, has been shown to viral transcript stabilization and productive virus infection in mammalian and mosquito cells (Sokoloski et al., 2010). For these reasons and binding nature of Hex1, I also speculate that FgV1 usurps cellular protein Hex1 to protect its viral mRNA from cellular mRNA decay machinery.

Future research should focus on investigating another function(s) of Hex1 protein in interaction with FgV1. The study is also required to understand the detailed molecular mechanisms of viral RNA translation and viral RNA stabilization.

LITERATURE CITED

- Ahlquist, P. (2006) Parallels among positive-strand RNA viruses, reverse-transcribing viruses and double-stranded RNA viruses. *Nat. Rev. Microbiol.* 4, 371-382.
- Ahlquist, P., Noueiry, A. O., Lee, W.-M., Kushner, D. B. and Dye, B. T. (2003) Host factors in positive-strand RNA virus genome replication. *J. Virol.* 77, 8181-8186.
- Arnold, K., Bordoli, L., Kopp, J. and Schwede, T. (2006) The SWISS-MODEL workspace: a web-based environment for protein structure homology modelling. *Bioinformatics*, 22, 195-201.
- Chu, Y.-M., Jeon, J.-J., Yea, S.-J., Kim, Y.-H., Yun, S.-H., Lee, Y.-W. and Kim, K.-H. (2002) Double-stranded RNA mycovirus from *Fusarium graminearum*. *Appl. Environ. Microbiol.* 68, 2529-2534.
- Dickson, A. M. and Wilusz, J. (2011) Strategies for viral RNA stability: live long and prosper. *Trends Genet.* 27, 286-293.
- Faruk, M. I., Eusebio-Cope, A. and Suzuki, N. (2008) A host factor involved in hypovirus symptom expression in the chestnut blight

- fungus, *Cryphonectria parasitica*. *J. Virol.* 82, 740-754.
- Galão, R. P., Chari, A., Alves-Rodrigues, I., Lobão, D., Mas, A., Kambach, C., Fischer, U. and Díez, J. (2010) LSm1-7 complexes bind to specific sites in viral RNA genomes and regulate their translation and replication. *RNA* 16, 817-827.
- Gao, K., Xiong, Q., Xu, J., Wang, K. and Wang, K. (2013) *CpBir1* is required for conidiation, virulence and anti-apoptotic effects and influences hypovirus transmission in *Cryphonectria parasitica*. *Fungal Genet. Biol.* 51, 60-71.
- Henderson, A. and Hershey, J. W. (2011) Eukaryotic translation initiation factor (eIF) 5A stimulates protein synthesis in *Saccharomyces cerevisiae*. *Proc. Nat. Acad. Sci. USA* 108, 6415-6419.
- Jackson, R. J., Hellen, C. U. and Pestova, T. V. (2010) The mechanism of eukaryotic translation initiation and principles of its regulation. *Nat. Rev. Mol. Cell Biol.* 11, 113-127.
- Jedd, G. and Chua, N. H. (2000) A new self-assembled peroxisomal vesicle required for efficient resealing of the plasma membrane. *Nat. Cell Biol.* 2, 226-231.
- Kim, K.-H. and Hemeway, C. (1996) The 5' nontranslated region of Potato virus X affects both genomic and subgenomic RNA synthesis. *J.*

Viol. 70, 5533-5540.

Kim, K.-H., Kwon, S.-J and Hemenway, C. (2002) Cellular protein binds to sequences near the 5' terminus of *Potato virus X* RNA that are important for virus replication. *Viol.* 301, 305-312.

Kwon, S.-J., Lim, W.-S., Park, S.-H., Park, M.-R. and Kim, K.-H. (2009) Molecular characterization of a dsRNA mycovirus, *Fusarium graminearum* virus-DK21, which is phylogenetically related to hypoviruses but has a genome organization and gene expression strategy resembling those of plant potex-like viruses. *Mol. Cells*, 28, 73-74.

Li, C. H., Ohn, T., Ivanov, P., Tisdale, S. and Anderson, P. (2010). eIF5A promotes translation elongation, polysome disassembly and stress granule assembly. *PLoS One* 5, e9942.

Mellits, K. H., Meredith, J. M., Rohll, J. B., Evans, D. J. and Almond, J. W. (1998) Binding of a cellular factor to the 3' untranslated region of the RNA genomes of entero-and rhinoviruses plays a role in virus replication. *J. Gen. Virol.* 79, 1715-1723.

Moon, S. L., Barnhart, M.D. and Wilusz, J. (2012) Inhibition and avoidance of mRNA degradation by RNA viruses. *Curr. Opin. Microbiol.* 15, 500-505.

- Park, M.-R., Park, S.-H., Cho, S.-Y. and Kim, K.-H. (2009) *Nicotiana benthamiana* protein, NbPCIP1, interacting with *Potato virus X* coat protein plays a role as susceptible factor for viral infection. *Viol.* 386, 257-269.
- Park, Y. W., Wilusz, J. and Katze, M. G. (1999) Regulation of eukaryotic protein synthesis: selective influenza viral mRNA translation is mediated by the cellular RNA-binding protein GRSF-1. *Proc. Nat. Acad. Sci. USA* 96, 6694-6699.
- Peat, T. S., Newman, J., Waldo, G. S., Berendzen, J. and Terwilliger, T. C. (1998) Structure of translation initiation factor 5A from *Pyrobaculum aerophilum* at 1.75 Å resolution. *Structure*, 6, 1207-1214.
- Polacek, C., Friebe, P. and Harris, E. (2009) Poly (A)-binding protein binds to the non-polyadenylated 3' untranslated region of dengue virus and modulates translation efficiency. *J. Gen. Virol.* 90, 687-692.
- Preiss, T. W. and Hentze, M. (2003) Starting the protein synthesis machine: eukaryotic translation initiation. *Bioessays*, 25, 1201-1211.
- Saini, P., Eyler, D. E., Green, R. and Dever, T. E. (2009) Hypusine-containing protein eIF5A promotes translation elongation. *Nature*, 459, 118-121.

- Scheller, N., Mina, L. B., Galão, R. P., Chari, A., Giménez-Barcons, M., Noueiry, A., Fischer, U., Meyerhans, A. and Díez, J. (2009) Translation and replication of hepatitis C virus genomic RNA depends on ancient cellular proteins that control mRNA fates. *Proc. Nat. Acad. Sci. USA* 106, 13517-13522.
- Shi, S. T. and Lai, M. (2006) HCV 5' and 3' UTR: When translation meets replication. *In: Hepatitis C Viruses: Genomes and Molecular Biology* (Tan, S. L. eds) pp. 49-88. Horizon Scientific Press, Norfolk.
- Sokoloski, K. J., Dickson, A. M., Chaskey, E. L., Garneau, N. L., Wilusz, C. J. and Wilusz, J. (2010) Sindbis virus usurps the cellular *HuR* protein to stabilize its transcripts and promote productive infections in mammalian and mosquito cells. *Cell Host Microbe*, 8, 196-207.
- Son, H., Seo, Y.-S., Min, K., Park, A. R., Lee, J., Jin, J.-M., Lin, Y., Cao, P., Hong, S.-Y., Kim, E.-K., Lee, S.-H., Cho, A., Lee, S., Kim, M.-G., Kim, Y., Kim, J. E., Kim, J.-C., Choi, G. J., Yun, S.-H., Lim, J. Y., Kim, M., Lee, Y.-H., Choi, Y.-D. and Lee, Y.-W. (2011) A phenome-based functional analysis of transcription factors in the cereal head blight fungus, *Fusarium graminearum*. *PLoS Pathog.* 7, e1002310.

- Son, M., Lee, K.-M., Yu, J., Kang, M., Park, J. M., Kwon, S.-J., and Kim, K.-H. (2013) The *HEX1* gene of *Fusarium graminearum* is required for fungal asexual reproduction and pathogenesis and for efficient viral RNA accumulation of *Fusarium graminearum* virus 1. *J. Virol.* 87, 10356-10367.
- Soundararajan, S., Jedd, G., Li, X., Ramos-Pamplona, M., Chua, N. H. and Naqvi, N. I. (2004) Woronin body function in *Magnaporthe grisea* is essential for efficient pathogenesis and for survival during nitrogen starvation stress. *Plant Cell*, 16, 1564-1574.
- Sun, Q., Choi, G. H. and Nuss, D. L. (2009) Hypovirus-responsive transcription factor gene *pro1* of the chestnut blight fungus *Cryphonectria parasitica* is required for female fertility, asexual spore development, and stable maintenance of hypovirus infection. *Eukaryot. Cell*, 8, 262-270.
- Wang, R. and Li, K. (2012) Host factors in the replication of positive-strand RNA viruses. *Chang Gung Med J.* 35, 111-124.
- Yuan, P., Jedd, G., Kumaran, D., Swaminathan, S., Shio, H., Hewitt, D., Chua, N.-H. and Swaminathan, K. (2003) A HEX-1 crystal lattice required for woronin body function in *Neurospora crassa*. *Nat. Struct. Mol. Biol.* 10, 264-270.

Zanelli, C. and Valentini, S. (2007) Is there a role for eIF5A in translation?

Amino Acids, 33, 351-358.

붉은 곰팡이 바이러스 1 과

상호작용하는 붉은 곰팡이의 *HEX1*

유전자에 대한 기능분석연구

손 문 일

초록

대표적인 식물 병원성 곰팡이인 붉은 곰팡이에서 분리·동정한 붉은 곰팡이 바이러스 1 (FgV1) 은 곰팡이에 감염하는 바이러스이다. FgV1 은 3' 말단의 poly (A) tail 을 제외하고 6,624 nucleotide 길이의 게놈으로 구성된다. 바이러스의 게놈은 53 nucleotide 의 5' 말단 비번역 부분, 46 nucleotide 의 3' 말단 비번역 부분을 가지며, 4 개의 open reading frame (ORF) 을 가진 것으로 추정된다. FgV1 은 붉은 곰팡이에 감염하여 형태학적인 측면, 생장과 발달, 대사와 병원성 등등 다양한 측면에서 기주 곰팡이의

생물학적 변화를 초래한다. FgV1 과 상호작용하여 이러한 변화를 초래하는 기주 인자를 찾기 위하여 단백질체 분석과 전사체 분석이 이루어졌다. 이러한 분석들을 통하여 곰팡이 단백질인 Hexagonal peroxisome protein (Hex1) 이 FgV1 감염 시에 과발현 되는 것을 확인하였다. Hex1 단백질은 peroxisome 에서 유래된 단백질로서 고밀도의 세포 소기관인 Woronin body 를 구성한다. Woronin body 는 곰팡이에게 가해지는 자극에 반응하여 세포벽에 존재하는 물질 이동 통로 septal pore 를 막는 역할을 한다. 본 연구에서는 Hex1 단백질의 기주 곰팡이 내에서의 다른 기능들을 구명하고 아울러 곰팡이 바이러스인 FgV1 에 특이적인 기능에 관하여 연구하였다. 먼저, Hex1 단백질의 기능을 연구하기 위하여 *HEX1* 유전자의 삭제 돌연변이체, 과발현 돌연변이체, complementation 돌연변이를 제작 한 후 FgV1 에 감염시켰다. *HEX1* 유전자의 삭제나 과발현이 FgV1 에 감염되지 않은 돌연변이체들에서는 vegetative growth 에 영향을 끼치지 않았지만, conidia 의 생성과 병원성을 감소시켰다. 또한, *HEX1* 삭제 돌연변이체의 균사를 절단하였을 때 세포질의 외부 유출이 일어나는 것을 확인하였다. 위의 현상들을 통하여, *HEX1* 은 붉은

곰팡이에서 asexual reproduction, pathogenesis, cellular integrity 유지에 중요한 역할을 하는 유전자임을 확인하였다. 앞선 결과와 다르게 FgV1 에 감염될 경우 vegetative growth 가 WT-VI 균주 보다 *HEX1* 유전자 삭제 돌연변이체에서는 증가, 과발현 돌연변이체에서는 증가하였다. 또한, 5 일째의 액체배지에서 배양한 균사와 고체배지에서 배양한 균주들에서 FgV1 RNA 의 accumulation 정도가 삭제 돌연변이체에서는 감소, 과발현 돌연변이체에서는 증가 하는 것을 확인하였다. 이러한 유전적 변이에 따른 FgV1 RNA accumulation 정도의 차이가 어떠한 기작에서 유래되는지를 확인하기 위하여 FgV1 과 Hex1 단백질간의 상호작용에 대한 심도 있는 연구를 수행하였다. 첫 번째로, 기존의 Hex1 protein 의 구조적 특성을 구명한 연구를 바탕으로 붉은 곰팡이의 RNA-binding fold 를 가지고 있는 Eukaryotic translational initiation factor 5A (IF-5A) 과 Hex1 protein 이 구조적으로 유사성의 높은 것을 확인하였다. 이러한 결과를 토대로, Electrophoretic mobility shift assay 를 통하여 Hex1 protein 이 *in vitro* 조건에서 FgV1 plus-strand RNA 의 5' 과 3' 비번역 부분에 특이적으로 결합하는 사실을 확인하였다. 또한, 이러한 특이적인

Hex1-FgV1 상호작용이 virus replication 을 촉진 하는 것을 붉은 곰팡이의 protoplast 에서 Northern blot 과 First-strand qRT-PCR 을 통하여 확인하였다. 본 연구를 통하여 붉은 곰팡이의 유전자와 단백질의 고유의 기능을 구명하였고, FgV1 과의 상호작용에서 Hex1 유전자의 특이적 기능을 통하여 앞으로의 곰팡이바이러스-기주 곰팡이 간의 상호작용 연구에 좋은 선례가 될 것으로 기대된다.

주요어: 붉은 곰팡이 바이러스 1 (*Fusarium graminearum virus 1*), 붉은 곰팡이, Hex1 단백질, 기주인자, RNA-단백질 결합, 바이러스 증식

학번: 2008-21357